

Overparametrized models with posterior drift*

Guillaume Coqueret[†] Martial Laguerre^{‡§}

July 1, 2025

Abstract

This paper investigates the impact of posterior drift on out-of-sample forecasting accuracy in overparametrized machine learning models. We document the loss in performance when the loadings of the data generating process change between the training and testing samples. This matters crucially in settings in which regime changes are likely to occur, for instance, in financial markets. Applied to equity premium forecasting, our results underline the sensitivity of a market timing strategy to sub-periods and to the bandwidth parameters that control the complexity of the model. For the average investor, we find that focusing on holding periods of 15 years can generate very heterogeneous returns, especially for small bandwidths. Large bandwidths yield much more consistent outcomes, but are far less appealing from a risk-adjusted return standpoint. All in all, our findings tend to recommend cautiousness when resorting to large linear models for stock market predictions.

*The authors would like to thank the participants of the 18th Financial Risks International Forum, the 7th QFFE event, the 29th Forecasting Financial Markets Conference, the 19th BiGSEM Doctoral Workshop, the Scientific Beta Alumni Global Summit, the 2025 AFFI conference, and the SAF lab seminar for their helpful comments.

[†]EMLYON Business School, 144 avenue Jean Jaurès, 69007 Lyon, FRANCE. E-mail: coqueret@em-lyon.com

[‡]EMLYON Business School, 144 avenue Jean Jaurès, 69007 Lyon, FRANCE. E-mail: laguerre@em-lyon.com

[§]Université Claude Bernard Lyon 1, Laboratoire de Sciences Actuarielle et Financière, 69007 Lyon, France.

1 Introduction

Recently, the literature in machine learning (ML) has investigated the notion of “*double descent*”, whereby linear overparametrized models (i.e., with more parameters than observations) can have surprising out-of-sample benefits.¹ As is customary in most machine learning contributions, including on double descent, a key assumption to derive analytical results is the invariance in distributions between the training and testing phases: the data generating process (DGP) is assumed to remain the same once the model has been calibrated. Unfortunately, this may not be the case in practice, especially in financial markets which can be subject to sudden regime changes. If we write $P_{y,X} = P_{y|X}P_X$ for the joint law of X and y , we see that there are potentially two drivers for the change of distribution in the DGP: the conditional one, $P_{y|X}$, and the unconditional one, P_X . When the law of X changes, we refer to *covariate shift*, whereas when the link between X and y evolves, we will talk of *posterior drift* (sometimes also referred to as *concept drift*, see, e.g. [Gama et al. \(2014\)](#) and [Lu et al. \(2018\)](#)). Interestingly, the notion of posterior drift has also witnessed a surge in interest lately, in particular from the ML community (see, e.g., [Maity et al. \(2024\)](#), [Hu and Lin \(2025\)](#) and [Wang and Qiao \(2025\)](#)).

The goal of the present paper is to investigate how posterior drift can be detrimental to out-of-sample forecasting accuracy in the context of overparametrized models.² Our practical motivation originates in the seminal paper by [Kelly et al. \(2024\)](#) which argues that the performance of aggregate market timing with linear models increases with the number of parameters. Since complexity is the ratio between the number of parameters and the sample size, the authors conclude that complexity is virtuous for equity premium prediction. However, several contributions have since then challenged this point of view, all from different angles. For instance, [Berk \(2023\)](#) underlines the lack of financial grounding (equilibrium consistency), whereas [Cartea et al. \(2025\)](#) argue that the effect of noise is underestimated in [Kelly et al. \(2024\)](#). Indeed, as the number of factors (i.e., predictors) increases, the amount of noise may also increase, thereby impairing the models’ accuracy. [Nagel \(2025\)](#) demonstrates that the random Fourier feature (RFF) trick used to artificially increase the number of predictors in fact collapses to a low-complexity kernel ridge regression. Resorting to RFFs is also problematic because they often require in-sample rescaling that violates the shift-invariance property required in theoretical results ([Fallahgoul \(2025\)](#)). Finally, [Buncic \(2025\)](#) points to another important shortcoming: adding a constant in the set of predictors reverses the pattern and performance then decreases with complexity. As a consequence, it turns out that Sharpe ratios obtained with low dimensional predictors are much higher than those reported in [Kelly et al. \(2024\)](#) for large levels of complexity.

In focusing on the perils of regime changes, we shed light on another explanation of the ambiguous role of overparametrization in the forecasting efficiency of linear models. Indeed, we contend that the efficacy of complex models in equity premium prediction can be severely jeopardized by changing economic environments. In practice, the relationships that are inferred during the estimation phase may change due to unpredictable shocks, and, in this case, the out-of-sample precision of predictions can be substantially attenuated. Another representation of such phenomena can be made through the lens of the signal-to-noise ratio.

¹This is sometimes also referred to as “*benign overfitting*” ([Bartlett et al. \(2020\)](#)), or “*grokking*” ([Power et al. \(2022\)](#), [Varma et al. \(2023\)](#)), though these notions do not necessarily perfectly overlap.

²The topic of covariate shift is already partly covered in Section 5 of [Hastie et al. \(2022\)](#) (via what they call the misspecified case), so that the room for novel contributions on the matter is limited.

In the presence of posterior drift, the information from predictors wanes, and, when signals are too weak, recent results indicate that ridgeless estimators perform worse than models that ignore the data completely (see Theorem 2 in [Shen and Xiu \(2025\)](#) and Corollary 1 in [Fallahgoul \(2025\)](#) for instance).

Our contributions are twofold. First, in Section 2, we extend the misspecified isotropic results of [Hastie et al. \(2022\)](#) to the case of non-i.i.d. data and derive the expected return of a market-timing strategy when *posterior drift* is taken into account. Second, in Section 3, we corroborate our theoretical findings with Monte-Carlo simulations. Third, in Section 4, we empirically confirm the intuitions. We first provide in Section 4.2 new evidence of time-variation in links between predictors and aggregate returns (betas). We then replicate in Section 4.3 the study of [Kelly et al. \(2024\)](#) with some subtleties. We test their procedure over several sub-periods of 15 years (the horizon for a representative investor) and across a range of bandwidth parameters, which we define below.

Our results indicate strong discrepancies in both dimensions (periods and bandwidths). Plainly speaking, this means that even with the bandwidth chosen in [Kelly et al. \(2024\)](#), the performance can be either well above (e.g., +7% monthly in 2005-2019) or well below (+0.5% in 1975-1989) than the one that we report for the full sample (+4%). It is possible to reduce this uncertainty by increasing the bandwidth value, but in this case, the average return decreases invariably towards zero, making complexity much less appealing.

In sum, while it is likely that sophistication *can* bring value in forecasting models, our findings suggest that analysts who rely on overparametrized models should pay particular attention to the stability and sensitivity of performance in their backtests.

Notations. $n, p \in \mathbb{N}_{>0}$ and $q \in \mathbb{N}_{\geq 0}$ are large dimensional parameters, possibly tending to infinity. n is the number of observations and $p + q$ the number of independent variables in linear models. We use C and D (resp. τ) for arbitrary large (resp. small) positive constants. Let $\langle \cdot, \cdot \rangle$ stand for the scalar product, i.e. for any vectors $u, v \in \mathbb{R}^p$, $\langle u, v \rangle = u'v$. Denote by $\|\cdot\| = \|\cdot\|_2$ the Euclidean norm of vectors. For any matrix $A \in \mathbb{R}^{p \times p}$ and any vector $v \in \mathbb{R}^p$, we denote by $\|v\|_A = \sqrt{v'Av}$, a reweighted version of the Euclidean norm. Similarly, for any matrix $A \in \mathbb{R}^{p \times p}$ and any vector $v, u \in \mathbb{R}^p$, define $\langle u, v \rangle_A = u'Av$. We use $\|\cdot\|_{\text{op}}$ to denote the Euclidean 2-norm of a matrix, namely, for any matrix $A \in \mathbb{R}^{n \times p}$, $\|A\|_{\text{op}}$ is the largest singular value of A .

2 Theoretical grounding

2.1 Setup: misspecification *and* posterior drift

This paper pertains to large models which, as in most of the recent literature, are *linear*, see, e.g., [Bartlett et al. \(2020\)](#), and [Kelly et al. \(2024\)](#). [Hastie et al. \(2022\)](#) do cover some non-linear cases but the corresponding require very lengthy proofs which is why the present paper focuses on extending linear combinations of features. Henceforth, our modelling framework follows that of [Hastie et al. \(2022\)](#) closely. We assume a data generating process (DGP) of the form

$$\begin{aligned} ((x_i, w_i), e_i) &\sim P_{x,w} \times P_e, \quad i = 1, \dots, n \\ y_i &= x_i'\beta + w_i'\theta + e_i, \quad i = 1, \dots, n, \end{aligned} \tag{1}$$

where the n random draws are independent. $P_{x,w}$ is a distribution on \mathbb{R}^{p+q} with $\mathbb{E}[x_i] = 0$ and $\mathbb{E}[w_i] = 0$ and

$$\text{Cov}[(x_i, w_i)] = \Sigma = \begin{bmatrix} \Sigma_x & \Sigma_{xw} \\ \Sigma'_{xw} & \Sigma_w \end{bmatrix}.$$

P_e is a distribution on \mathbb{R} with zero mean and variance σ^2 . In our empirical application, as in [Kelly et al. \(2024\)](#), y will be the equity premium and x a set of macroeconomic predictors that are expected to have some predictive power over the premium.

The agent has access to the x_i but not to the w_i , and hence only sees an incomplete picture, this is why her model is labeled as *misspecified*. This corresponds to the assumptions in Section 5 of [Hastie et al. \(2022\)](#) and, to some extent, to Section IV of [Kelly et al. \(2024\)](#). We write $(y_i, x_i) \in \mathbb{R} \times \mathbb{R}^p$ for one observation in the training data, and (y, X) for the corresponding aggregated vector (in \mathbb{R}^n) and matrix (in $\mathbb{R}^{n \times p}$).

As in [Hastie et al. \(2022\)](#), we define out-of-sample prediction risk of the well specified model, i.e. the model in which all the covariates are observed, as

$$R_X(\hat{\beta}, \beta) := \mathbb{E}[(x'_0(\hat{\beta} - \beta))^2 | X] = B_X(\hat{\beta}, \beta) + V_X(\hat{\beta}, \beta), \quad (2)$$

where x_0 is a random draw of P_x that is independent from the training data. In the equation, the **bias** is $B_X(\hat{\beta}, \beta) = \|\mathbb{E}[\hat{\beta} | X] - \beta\|_{\Sigma}^2$, and the **variance** is $V_X(\hat{\beta}, \beta) = \text{Tr}[\text{Cov}(\hat{\beta} | X)\Sigma]$.

The main departure from existing results is that we now discriminate between the (β', θ') vector that is used for the two data generating processes in Equation (1): one vector for the training data $((\beta'_{\text{is}}, \theta'_{\text{is}})')$ and another one for the testing data $((\beta'_{\text{oos}}, \theta'_{\text{oos}})')$. In doing so, we include **posterior drift** in the model: we postulate a change in the link between y and $(x', w)'$. Empirical support for this assumption will be provided in Section 4.2 below.

The estimator $\hat{\beta}$ is evaluated with the in-sample (is) or out-of-sample (oos) generated data:

$$\hat{\beta}_u := \hat{\beta}_u(z_n) = (X'X + \alpha I)^{-1} X'(X\beta_u + e) = n^{-1}(\hat{\Sigma} + z_n I)^{-1} X'(X\beta_u + W\theta_u + e), \quad (3)$$

where $\alpha > 0$ and $u \in \{\text{is}, \text{oos}\}$. Crucially, the above estimator relies on shrinkage with intensity $z_n = \alpha/n$ towards the identity matrix. In the remainder of the paper, we omit the dependence of the regularization parameter on the sample size n and set $z := z_n$. If $n < p$ and $z \rightarrow 0$, the pseudo-inverse is taken for the inverse matrix. We have also set $\hat{\Sigma} = X'X/n$. Below, we explicit the terms for the quadratic error (2) that is made when using the estimator $\hat{\beta}_{\text{is}}$ (from the data generated with β_{is}) when compared to the changed (or realized) β_{oos} . We are interested in this subsection in results for ridgeless estimators (when $z \rightarrow 0^+$).

Proposition 1. *Under model (1) and with $z \rightarrow 0$, the prediction risk of the misspecified model is*

$$\begin{aligned} R_X^m(\hat{\beta}_{\text{is}}, \beta_{\text{oos}}, \theta_{\text{oos}}) &= \mathbb{E}[(x'_0(\hat{\beta}_{\text{is}} - \beta_{\text{oos}}) - w'_0\theta_{\text{oos}})^2 | X] \\ &= R_X(\hat{\beta}_{\text{is}}, \beta_{\text{oos}}) + M(\theta_{\text{oos}}), \end{aligned}$$

where $M(\theta_{\text{oos}}) = \mathbb{E}[(w'_0\theta_{\text{oos}} - \mathbb{E}[w'_0\theta_{\text{oos}} | x_0])^2]$ is the misspecification bias, i.e., the signal embedded in the unobserved features (following the notation of [Hastie et al. \(2022\)](#)). Moreover, in the isotropic case $\Sigma = I$,

$$\lim_{n,p \rightarrow \infty} R_X^m(\hat{\beta}_{\text{is}}, \beta_{\text{oos}}, \theta_{\text{oos}}) = \begin{cases} (\sigma^2 + \|\theta_{\text{is}}\|_2^2) \frac{c}{1-c} + \|\beta_{\text{oos}} - \beta_{\text{is}}\|_2^2 + \|\theta_{\text{oos}}\|_2^2 & p/n \rightarrow c < 1 \\ (\sigma^2 + \|\theta_{\text{is}}\|_2^2)(c-1)^{-1} + c^{-1}\|\beta_{\text{is}} - \beta_{\text{oos}}\|_2^2 & p/n \rightarrow c > 1 \\ + (1-c^{-1})\|\beta_{\text{oos}}\|_2^2 + \|\theta_{\text{oos}}\|_2^2. & \end{cases} \quad (4)$$

The proof of the proposition is postponed to Appendix A.4. The limiting expressions generalize Theorem 4 in [Hastie et al. \(2022\)](#) by adding the posterior drift component. Plainly, both expressions for the risk are increasing in the **misspecification risk** $\|\theta_{oos}\|_2^2$ due to the unobserved features *and* in the **drift risk** $\|\beta_{is} - \beta_{oos}\|_2^2$ that comes from the change in loadings.

2.2 Portfolio performance under posterior drift

Proposition 1 quantifies the impact of the presence of posterior drift on the risk of out-of-sample prediction of linear (ridge) regressions in the over-parameterized setting. We now focus on the impact on the financial performance of a market timing strategy. As in [Kelly et al. \(2024\)](#), we analyze the returns of the strategy which consists of adjusting the position in an asset according to its estimated expected returns. Formally, the strategy's return can be written as

$$r_{t+1}^{(s)}(z) = \hat{\pi}_t(z)r_{t+1}, \quad (5)$$

where $\hat{\pi}_t(z) = \sum_{k=1}^p \hat{\beta}_{is}^{(k)}(z)x_t^{(k)}$ is the adjusted position in the asset and r_{t+1} is its realized monthly return (the superscript (s) in the notation stands for *strategy*). The estimated loadings in this case can be shrunk as in the general case in Equation (3).

For brevity, we directly consider the misspecified framework described in (1) and without loss of generality, we assume $\sigma^2 = 1$. We provide similar results within the well-specified framework in Appendix A.5.1 and A.5.2.

The following assumption establishes the linear model from which the covariates are considered to be drawn.

Assumption 2.1. The covariates have the form $x_i = \Sigma^{1/2}z_i$ with $z_i = (z_{i1}, z_{i2}, \dots, z_{ip})$ having independent and identically distributed entries. Moreover, for all $j \in \{1, \dots, p\}$, $\mathbb{E}[z_{ij}] = 0$, $\mathbb{E}[z_{ij}^2] = 1$ and $\mathbb{E}[|z_{ij}|^{4+a}] \leq C < \infty$ for $a > 0$.

The out-of-sample expected return of the timing strategy under posterior drift can be decomposed as follows.

Proposition 2. *Let $z > 0$, $\xi = (e_1, e_2, \dots, e_n)'$ with $(e_i)_i$ as in (1) and Assumption (2.1) hold. Furthermore, denote by $r_{t+1}^{(s,w)}(z)$ the return of the strategy if the model is well-specified, i.e. there are no unobserved features, w_i , in the DGP (1). Then,*

$$\mathbb{E} \left[r_{t+1}^{(s)}(z) \middle| X \right] = \mathbb{E} \left[r_{t+1}^{(s,w)}(z) \middle| X \right] + \mathcal{M}(z) \quad (6)$$

where

$$\begin{aligned} \mathbb{E} \left[r_{t+1}^{(s,w)}(z) \middle| X \right] &= \beta'_{oos} \Sigma_x (zI + \hat{\Sigma}_x)^{-1} \left(\hat{\Sigma}_x \beta_{is} + \frac{1}{n} X' \xi \right) \\ \mathcal{M}(z) &= \left(\beta'_{oos} \Sigma_x + \theta'_{oos} \Sigma'_{xw} \right) (zI + \hat{\Sigma}_x)^{-1} \mathbb{E} \left[\hat{\Sigma}_{xw} \middle| X \right] \theta_{is} \\ &\quad + \theta'_{oos} \Sigma'_{xw} (zI + \hat{\Sigma}_x)^{-1} \left(\hat{\Sigma}_x \beta_{is} + \frac{1}{n} X' \xi \right). \end{aligned}$$

The proof is postponed to Section A.5.3 in the Appendix. The proposition shows that the out-of-sample expected return of the timing strategy under posterior drift crucially depends on the interactions between the observed and the unobserved covariates. These complex relations are encapsulated in the quantity $\mathcal{M}(z)$. Therefore, in order to provide more qualitative qualitative insights and intuition, we study different models of interest that allow to make this term more explicit.

In what follows, we study the simpler case of i.i.d. features with unit variance, which entails $\Sigma = I$.

We consider the following dimensional ratios.

Assumption 2.2. For some $\tau > 0$, $\tau \leq c\phi \leq \tau^{-1}$, with $c = (p + q)/n$, $\phi = p/(p + q) \in (0, 1]$.

This assumption is standard in statistical theory and characterizes the proportional regime in which our study takes place. The constant c stands for the complexity of the true models while ϕ is the misspecification ratio. The product $c\phi$ is the complexity of the misspecified model.

The following proposition gives the limiting out-of-sample expected return of the timing strategy under posterior drift and i.i.d. features, $\mathcal{E}^{(d)}(z; c\phi)$. Moreover, we introduce an important benchmark, namely the limiting zero-drift expected return from Proposition 3 in Kelly et al. (2024):

$$\mathcal{E}(z; c\phi) = \lim_{\substack{n, p \rightarrow \infty \\ p/n \rightarrow c\phi}} \mathbb{E} \left[r_{t+1}^{(s)}(z) \middle| X, \beta_{is} = \beta_{oos} \right]. \quad (7)$$

Proposition 3. Let $z > 0$ and assume $(x_i, w_i)'$ has independent and identically distributed entries with unit variance and finite moments of order $4 + a$, for some $a > 0$. Then,

$$\mathbb{E} \left[r_{t+1}^{(s)}(z) \middle| X \right] \xrightarrow[\substack{n, p \rightarrow \infty \\ p/n \rightarrow c\phi}]{\mathbb{P}} f(z; c\phi) \langle \beta_{is}, \beta_{oos} \rangle = \mathcal{E}^{(d)}(z; c\phi), \quad (8)$$

where $f(z; c\phi)$ and $f(c\phi) := \lim_{z \rightarrow 0} f(z; c\phi)$ are defined in Equations (39) and (49) in the Appendix.³

In particular, if $\|\beta_{is}\|^2 = \|\beta_{oos}\|^2$, then

$$\mathbb{E} \left[r_{t+1}^{(s)}(z) \middle| X \right] \xrightarrow[\substack{n, p \rightarrow \infty \\ p/n \rightarrow c\phi}]{\mathbb{P}} \mathcal{E}^{(d)}(z; c\phi) = \mathcal{E}(z; c\phi) - \frac{1}{2} f(z; c\phi) \|\beta_{is} - \beta_{oos}\|^2,$$

Furthermore, $z \mapsto f(z; c\phi) \langle \beta_{is}, \beta_{oos} \rangle$ is monotone decreasing (resp. increasing) in z when $\langle \beta_{is}, \beta_{oos} \rangle \geq 0$ (resp. $\langle \beta_{is}, \beta_{oos} \rangle \leq 0$).

This proposition, the proof of which is located in Section A.5.4, calls for several remarks. First, the above expression generalizes the results of Kelly et al. (2024). Indeed, the above formulation allows to recover Figure 5 in their theoretical section when setting $c = 10$ and $\beta = \beta_{is} = \beta_{oos}$ with $\beta_i = \beta_j$ for any $i, j \in \{1, \dots, p\}$ and such that $\|\beta\|^2 = 0.2$ when $q = 0$. The

³Propositions 4 and 8 in the Appendix provide non-asymptotic bounds (under stronger conditions) for the approximation of the expected return. However, these bounds are additive in the errors and, therefore, not relative to the scale of the return. Hence, given the typical order of magnitude of financial returns, it would make sense to establish multiplicative bounds similar to those developed by Cheng and Montanari (2022), Misiakiewicz and Saeed (2024) or Defilippis et al. (2024) for the approximation of the test error of different types of ridge regression. We leave this avenue open for further research.

pattern exhibited in Kelly et al. (2024) is a special case when the scalar product $\langle \beta_{is}, \beta_{oos} \rangle$ is fixed to a particular value.

The shape in the r.h.s. of (8) is a multiple of the scalar product $\langle \beta_{is}, \beta_{oos} \rangle$. Simply put, the expected performance is proportional to the alignment between the in-sample loadings and the out-of-sample ones. Given the fact that the mean of the estimated loadings is very close to zero (upon the Random Fourier transform), the scalar product can also be interpreted as the sample correlation between β_{is} and β_{oos} . In particular, if the two vectors are orthogonal (with null correlation), then the average return is simply zero. This makes sense, as it is in this case impossible to extract any meaningful information from the training set.

The proportional form in (8) is in fact very general and can also be obtained with a DGP that includes latent features, as in Hastie et al. (2020). The corresponding results and proofs are postponed to Appendix A.5.5.

Remark 1. *The limiting expression in (8) can be adapted to any specific form of β_{oos} . For instance, let β_{oos} be a linear transformation of β_{is} , i.e. $\beta_{oos} = W\beta_{is}$ with $W \in \mathbb{R}^{p \times p}$ deterministic. If we denote by $(\xi_k)_{1 \leq k \leq p}$ the eigenvalues of W and $(v_i)_{1 \leq k \leq p}$ their associated eigenvectors, then the (asymptotic) expected return of the strategy converges to*

$$\mathcal{E}^{(d)}(z; c\phi) = h(z; c\phi, \beta_{is}, W) \|\beta_{is}\|^2,$$

where $h(z; c\phi, \beta_{is}, W) := f(z; c\phi) \sum_{k=1}^p \xi_k \text{cosim}(\beta_{is}, v_k)^2$ and $\text{cosim}(\beta_{is}, v_k) := \langle \beta_{is}, v_k \rangle / \|\beta_{is}\|$ is the cosine similarity between β_{is} and v_k , which lies between -1 and 1 . In the Appendix, we also show that $f \in [0, 1]$, thus it is straightforward that $\mathcal{E}^{(d)}(z; c\phi) \geq 0$ if W is positive semidefinite. Otherwise, if W is not positive semidefinite, the picture is more nuanced and the expected return can be negative.

More importantly, when the covariates are isotropic, the misspecification term $\mathcal{M}(z)$ in (6) vanishes, and the out-of-sample expected return behaves as if the model was well-specified with a true complexity equal to $c\phi = p/n$. This result leads us to draw the following remark which establishes the conditions under which the presence of posterior drift deteriorates the expected returns of the market-timing strategy.

Remark 2. *Let $z > 0$ and assume that $(x_i, w_i)'$ has independent and identically distributed entries with unit variance and finite moments of order $4 + a$, for some $a > 0$. Then,*

$$\mathcal{E}^{(d)}(z; c\phi) < \mathcal{E}(z; c\phi)$$

if and only if

$$\langle (\beta_{oos} - \beta_{is}), \beta_{is} \rangle < 0, \tag{9}$$

or alternatively, if and only if,

$$\|\beta_{oos}\|^2 - \|\beta_{is}\|^2 < \|\beta_{is} - \beta_{oos}\|^2. \tag{10}$$

Consequently, the loss of financial performance depends on the scalar product between the vector of *in-sample* regression coefficients, β_{is} , and a *residual* vector, $\beta_{oos} - \beta_{is}$, arising from the change in DGP. In particular, when the amount of signal contained in the first p features is preserved or is less important *out-of-sample* than *in-sample*, i.e. $\|\beta_{oos}\|^2 \leq \|\beta_{is}\|^2$, Remark

2 implies that the presence of posterior drift not only increases the out-of-sample prediction risk (as documented in our first proposition), but, more interestingly from a financial standpoint, it also systematically deteriorates the returns of market timing strategies based on these predictions.

3 Simulations

The proofs of Propositions 2 and 3 are somewhat cumbersome. This section is dedicated to the verification of these theoretical results via Monte-Carlo simulations. To this end, we generate data as per the DGP of Equation (1). Let $p + q = 300$. We draw $n = 100$ samples of covariates from a 300-dimensional standard multivariate normal distribution, i.e. $(x_i, w_i) \sim N(0, \Sigma)$ with $\Sigma = I_{300}$. The error term is a white Gaussian noise, viz. $e_i \sim N(0, 1)$.

The *in-sample* and *out-of-sample* true parameters vectors for the observed data, β_{is} and β_{oos} respectively, are equally distributed on the eigenvectors of Σ , namely, on the canonical basis vectors.⁴ β_{is} has unit signal, that is $\|\beta_{is}\|^2 = 1$, while we consider a sequence of $(\beta_{oos,k})_k$ with decreasing signal. In particular, $\beta_{is} = p^{-1/2}(1, 1, \dots, 1, 1)'$ and $\beta_{oos,k} = kp^{-1/2}(1, 1, \dots, 1, 1)'$ with $k \in \{0.2, 0.4, 0.6, 0.8, 1\}$, which yields $\|\beta_{oos,k}\|^2 = k^2 \leq 1$ and $\langle \beta_{is}, \beta_{oos} \rangle = k$.

We analogously generate the true parameters vectors for the unobserved data, θ_{is} and θ_{oos} , setting only a different number of coefficients, viz. q instead of p . Thus, the signal of the model *in-sample* is always equal to 2 while it is set to $2k^2$ *out-of-sample*, for $k \in \{0.2, 0.4, 0.6, 0.8, 1\}$. Finally, we simulate the performance of two market-timing strategies based on ridge estimators with shrinkage intensity $z \in \{0.01, 0.1\}$.

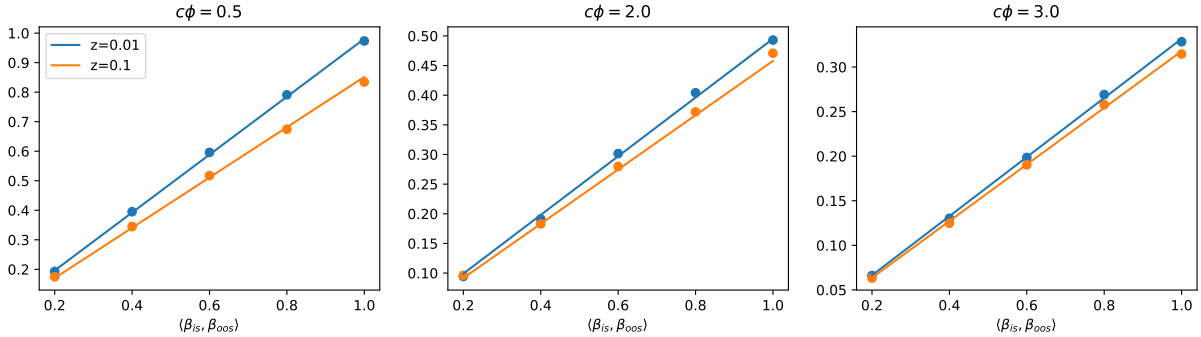


Figure 1: Simulated and theoretical returns of the strategy under mild regularization. The model’s true complexity is $c = 3$ ($p + q = 300$, $n = 100$). z is the regularization parameter of the ridge estimator. We plot the theoretical returns of the strategy as per Proposition 3 (solid line). Simulated returns (dots) are generated according to the process described in Section 3 and are averaged over 100,000 random draws.

As expected from Proposition 3, the strategy’s expected return is linear in the scalar product of β_{is} and β_{oos} . This is verified in Figure 1. This pattern arises whether the model is misspecified and underparameterized (Fig. 1, left), misspecified and overparameterized (Fig. 1, center) or well-specified (Fig. 1, right). Note that the rightmost point on each plot corresponds to the expected return in the no-drift scenario.

⁴In Appendix A.2, we perform the same analysis considering true parameters vectors concentrated on some directions of Σ .

We defer the comparison of simulated and theoretical expected returns of the market-timing strategy under strong regularization ($z \in \{10, 100\}$) to Appendix A.1. And, once again, these experiments confirm the claims stated in Proposition 3.

4 Empirical evidence

4.1 Data

We rely on the same data as Kelly et al. (2024), which comes from Goyal et al. (2024) and is available on Amit Goyal’s website. We use the CRSP value-weighted returns minus the T-bill rate as dependent variable. The predictors consist of the 14 macro-economic indicators used in Kelly et al. (2024), to which we add lagged returns.

In Section 4.2, we will compute betas from predictive regressions:

$$r_{t+1} = a + \sum_{k=1}^p \beta^{(k)} x_t^{(k)} + e_{t+1}, \quad (11)$$

where the $x_t^{(k)}$ are all p predictors. We estimate $\hat{\beta}$ every month on rolling windows of 15 years (180 points), which is our reference horizon. This generates time-series of loadings $\hat{\beta}_t$ that characterize the predictive link between the predictors and the returns from the CRSP portfolio r_{t+1} . These series are plotted in Figure 2 below and therein we have included lagged returns up to order 6.

4.2 Time-varying betas

There is considerable evidence supporting the time-varying nature of the coefficients in asset pricing models. Such effects have been documented on the performance of **predictive regressions** (Dangl and Halling (2012), Coulombe (2023), Farmer et al. (2023)), in **factor models** (Ghysels (1998), Bollerslev et al. (2024)) and for **risk premia estimation** in particular (Gagliardini et al. (2016), Bakalli et al. (2023)).

Empirically, this stylized fact can be revealed by change point detection. Such techniques seek to uncover sharp changes in the distribution of ordered observations (time series). They can take two forms, parametric and non-parametric. Parametric change point detection constrains the model to learn a particular functional form, i.e., observations between the change points are assumed to be drawn from a specific family of distribution (see Frick et al. (2014), Roy et al. (2016), Enikeeva and Harchaoui (2019)). This assumption is relaxed in the case of non-parametric change point detection and we refer to Aminikhanghahi and Cook (2017) for a complete survey on change point detection applied to time series. Recent contributions evaluate the dissimilarity of distributions using kernel distances (Garreau and Arlot (2018), Arlot et al. (2019)) or rank (Lung-Yut-Fong et al. (2015)).

We choose to rely on the multivariate nonparametric multiple change point detection method recently proposed by Londschien et al. (2023) and that builds upon the use of classifiers. Notably, this will allow us to study betas in a joint manner: the entire time series structure of the coefficients is used to detect change points. Specifically, our analysis of time-

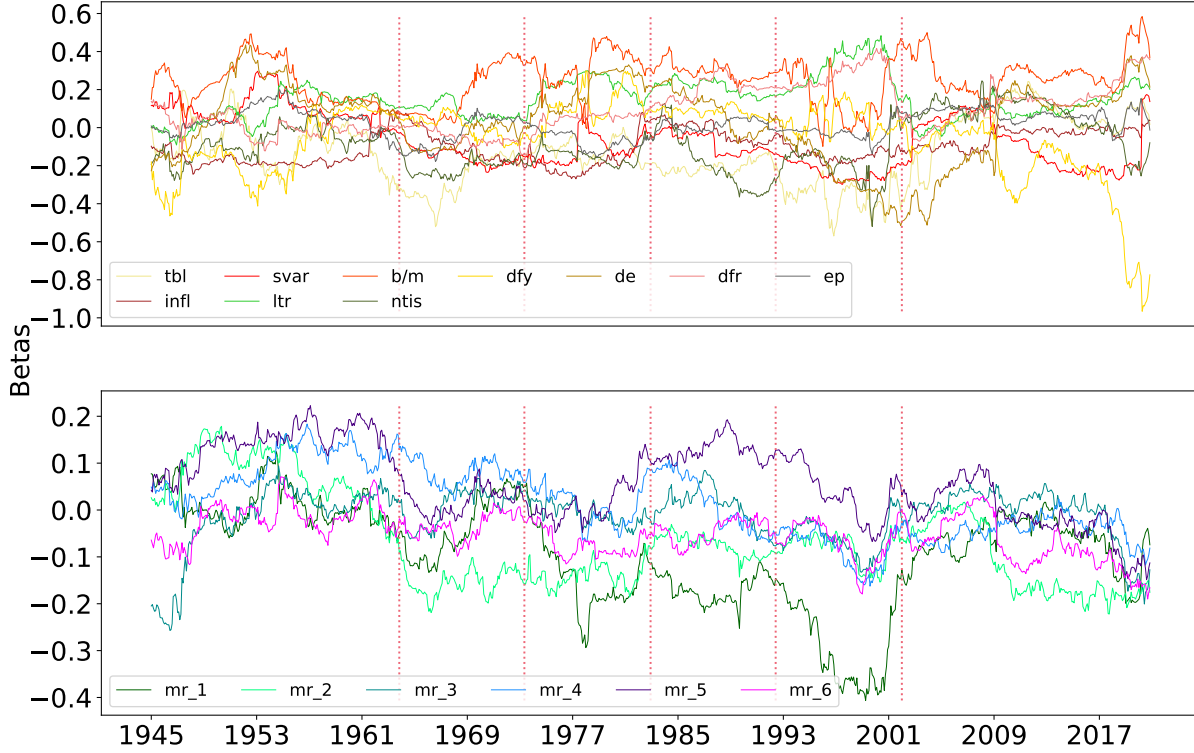


Figure 2: Time series of the betas. Each month, we plot the coefficients of the linear time series regressions of the returns onto each predictor (the $\hat{\beta}^{(k)}$ in Equation (11)). Estimations are performed on a fifteen-year rolling window. mr_i denotes the i -month lagged marked return. Returns and predictors are standardized following the protocol of Kelly et al. (2024) (Section V). Change point estimates (see Section 4.2) are represented by red (vertical) dashed lines.

variation is carried out with random forests via the *changeforest* algorithm⁵ whose technicalities we briefly outline below.

The idea behind the algorithm is to determine recursive binary splits at the points maximizing the nonparametric classifier log-likelihood ratio. This is shown in Figure 3.⁶ Therein, we have fed the time-series of the betas (the $\hat{\beta}_t^{(p)}$ from Figure 2) to *changeforest*.⁷ The top panel of the graph shows that the most relevant split occurs in December 1982. It is the one that maximizes the gain of the classifier when deciding between two regimes (two classes). The second horizontal panel show the following two splits, in November 1963 and January 2002. Lastly, the bottom panel provides three new splits. Indeed, we see that the first and last periods are not split in two because the corresponding tests were not conclusive. This

⁵The repository is available at <https://github.com/mlondschien/changeforest.git>

⁶We stick to the default hyperparameters of the algorithm with two exceptions. First, we set the maximum tree depth to 2 since, by default, $p^{1/2} = 4$ features are selected for each tree. Second, we arbitrarily choose a minimal relative segment length of 0.125 so the results appear sparser. By setting a smaller minimum relative length, the algorithm detects an abundance of change points.

⁷We exclude the variables "lty", "dp", "dy" and "tms" from the regressions as they introduced too much multicollinearity, yielding some estimates to be overly positive while others compensating with large negative values.

procedure tests if the split significantly improves the gain of the classifier. When the gain is too marginal, the algorithm stops, as for the pruning of simple decision trees. The final result clearly identifies several break points in the time-series of loadings, which justifies our assumption that changes occur between the training (in-sample) phase and the testing (out-of-sample) stage.

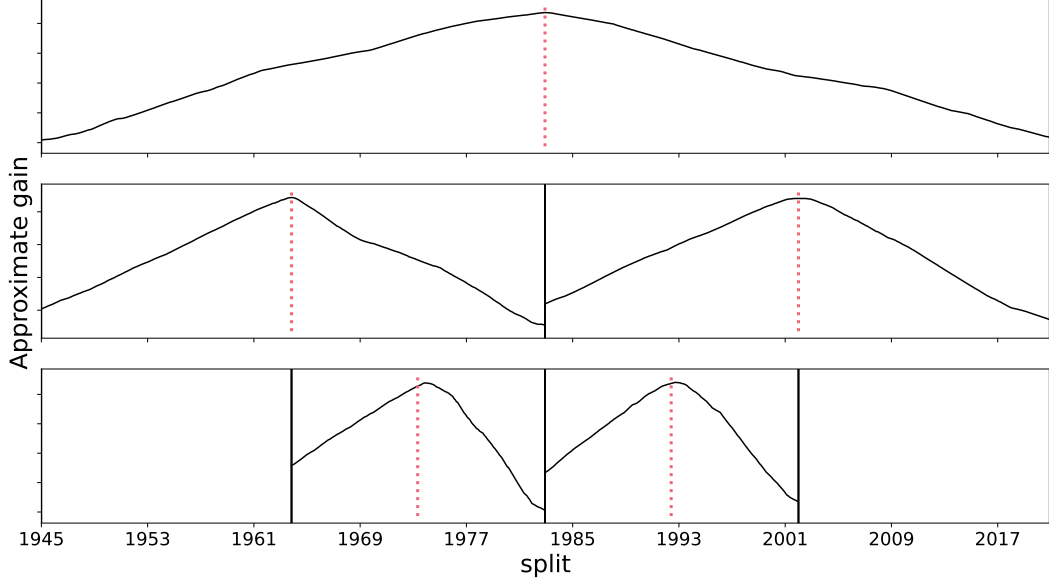


Figure 3: Change point detection. We plot the approximate gain curves from the last step of the two-step search for the three binary segmentations obtained with the *changeforest* algorithm (Londschien et al. (2023)). Change point estimates are marked with vertical red dots.

4.3 Protocol

We now closely follow the empirical protocol of Kelly et al. (2024) and we keep the notations therein. The idea is to model aggregate returns as a linear function of a large number of predictors which are created from a smaller set of macro-economic indicators, namely those analyzed in Welch and Goyal (2008). To expand the predictor space, Kelly et al. (2024) resort to Random Fourier Features (RFFs). More precisely, if G_t is the 15×1 vector of the original predictors, we will use

$$S_{i,t} = \frac{1}{\sqrt{p}} [\sin(\gamma w_i' G_t), \cos(\gamma w_i' G_t)], \quad w_i \stackrel{d}{=} \mathcal{N}(O, I_{15}) \quad (12)$$

as our independent variables in the predictive regression $r_{t+1} = S_{i,t}' \beta_i + e_{t+1}$. Importantly, i is the index of a random draw of the stochastic weights w_i , which are i.i.d. Because the predictors will be random, it is important to cancel the noise by averaging across many independent draws of w_i - usually several hundreds. Moreover, we are interested in the overparametrized regime, hence all our results below pertain to the case $n = 12$ and $p = 600$, so that the complexity level is equal to $c = 50$. In Kelly et al. (2024), the benefits from complexity vanish theoretically for $c > 10$ and empirically for $c > 50$. This is why we henceforth work with a high and fixed level of complexity $c = 50$.

In Equation (12), an important parameter is γ , the bandwidth of the kernel, which determines the level of nonlinearity of the model induced by the RFFs. In Kelly et al. (2024), the authors show that their approach is insensitive to this choice, at least when γ lies between 0.5 and 2. Our findings below paint a more nuanced picture.

Each month, given a random draw w_i and the features from Equation (12), we estimate the $\hat{\beta}$ as

$$\hat{\beta}_i^{RF}(z) = \left(zI + n^{-1} \sum_{t=1}^n S_{i,t} S_{i,t}' \right)^{-1} \frac{1}{n} \sum_{t=1}^n S_{i,t} R_{t+1}, \quad (13)$$

where RF stands for "random features" and $z > 0$ is a regularization parameter which ensures that the inverse matrix is well defined when the number of predictor exceeds the sample size n . The weight assigned to the market portfolio is then simply this estimator defined above and the corresponding realized return is evaluated after one month. The procedure is then repeated until the end of the sample and monthly returns are averaged over alternative periods of time.

For comparison purposes, we also report the average returns of the strategy when the raw features, G_t , are used to compute the the position, instead of the RFFs, $S_{i,t}$. The portfolio weight of this strategy is hence given by

$$\hat{\beta}^L(z) = \left(zI + n^{-1} \sum_{t=1}^n G_t G_t' \right)^{-1} \frac{1}{n} \sum_{t=1}^n G_t R_{t+1}, \quad (14)$$

where the superscript L stands for "linear". In Figure 4, the corresponding returns are shown with horizontal dashed lines (they do not depend on γ).

4.4 Results: sensitivity to bandwidths and periods

In Figure 4, we plot the average return obtained when using $\hat{\beta}_i^{RF}(z)$ as portfolio weight - averaged across 500 draws of w_i . We average returns over periods of 15 years for two reasons. First, because 15 years is already a long horizon for an investor and second because this allows to span several types of economic conditions: both periods of growth and slowdown. The values are reported for two levels of regularization: $z = 0.01$ (left) and $z = 100$ (right).

For a small regularization ($z = 0.01$) and $\gamma = 2$, as in the original paper, the return for the period 2005-2019 is 7.24% but it shrinks to 0.52% for 1975-1989 - a reduction by a factor 14. An analyst in 1974 would probably choose $\gamma = 1$ (from the red curve with $z = 0.01$), and hope for a return of 5%. But the performance in the following 15 years would prove very disappointing (less than 1%: again, a significant contraction).

For the sake of completeness, we also depict the sensitivity of the annualized Sharpe ratio in Figure 5. Over the full sample, we find a maximum value of 0.3, slightly lower than the roughly 0.4 reported by Kelly et al. (2024) in their Figure 8 (Panel A). These values are somewhat underwhelming if we put them in perspective with the 0.44 Sharpe ratio of the excess returns on the market index documented in Pav (2021) over the 1926-2020 period - from the Ken French data library. For the raw market portfolio, when the risk-free rate is not subtracted, the Sharpe ratio increases to 0.62. This is even before taking trading costs into account: holding the market portfolio entails minimum trading costs, which is not the case of the timing strategy presented in Kelly et al. (2024).

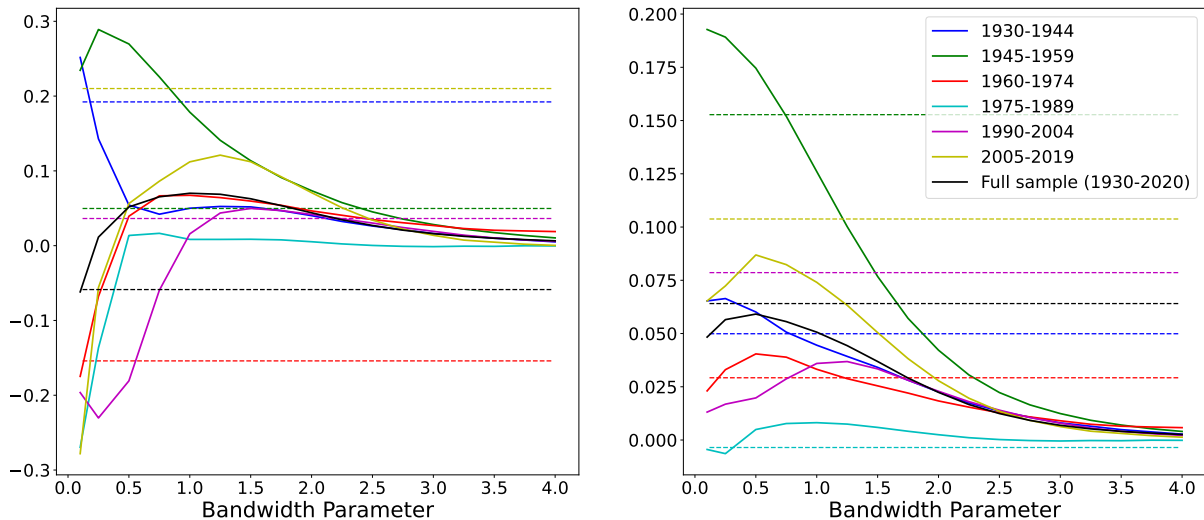


Figure 4: Returns' sensitivity to periods and bandwidth. We plot average realized returns obtained on six sub-periods and on the full sample (solid lines) for $p = 600$ RFFs, as a function of the bandwidth parameter of the kernel from the Random Fourier Features. The (dashed) horizontal lines display the return of the strategy when the raw features are used instead of RFFs. In this case, $p = 15$. For the sake of visibility, we do not plot the return of the strategy when using raw features for the 1975-1989 period (-50%). The left plot shows the case when the penalization parameter is $z = 0.01$ (mild regularization), while the right one pertains to $z = 100$ (strong regularization). Portfolios are averaged over 500 random draws.

In fact, a closer look reveals the unreasonably high levels of volatility that are implied by these Sharpe ratios. A monthly return of 0.03 (reported both in Figure 4 and in Kelly et al. (2024) for a bandwidth of two) translates arithmetically to 0.36 on an annual basis, thus a Sharpe ratio of 0.3 suggests a yearly volatility above 100%, which is prohibitively high, even for risk-prone investors (e.g., hedge funds).

Lastly, Figure 5 overwhelmingly indicates that the best choice of bandwidth is indeed close to two. Except for one period (posterior to World War II), all curves reach their maximum when the bandwidth is in the vicinity of two. This is a stable and consistent pattern - which may explain why it is presented as the baseline case in Kelly et al. (2024).

4.5 Time-varying bandwidths

In Figure 4, we note that the optimal choice of γ is time-varying. It lies between $\gamma^* = 0$ in the first period (left graph) or in the second period (right graph) and $\gamma^* = 1.5$ in 1990-2004 or 2005-2019 (left panel) and in 1990-2004 (right panel). Choosing larger values for γ reduces uncertainty, but at the cost of lower returns.

We now want to account for the fact that investors can adjust γ based on past performance. In a new exercise, we pick, for a given period of 15 years, the bandwidth that yielded the best results in the previous period (we call this the “feasible” strategy), but also the bandwidth that proved the best ex-post, i.e., in *hindsight*. The corresponding returns are gathered in Table 1.

As expected, when γ is chosen in hindsight (rightmost columns), the strategy based on

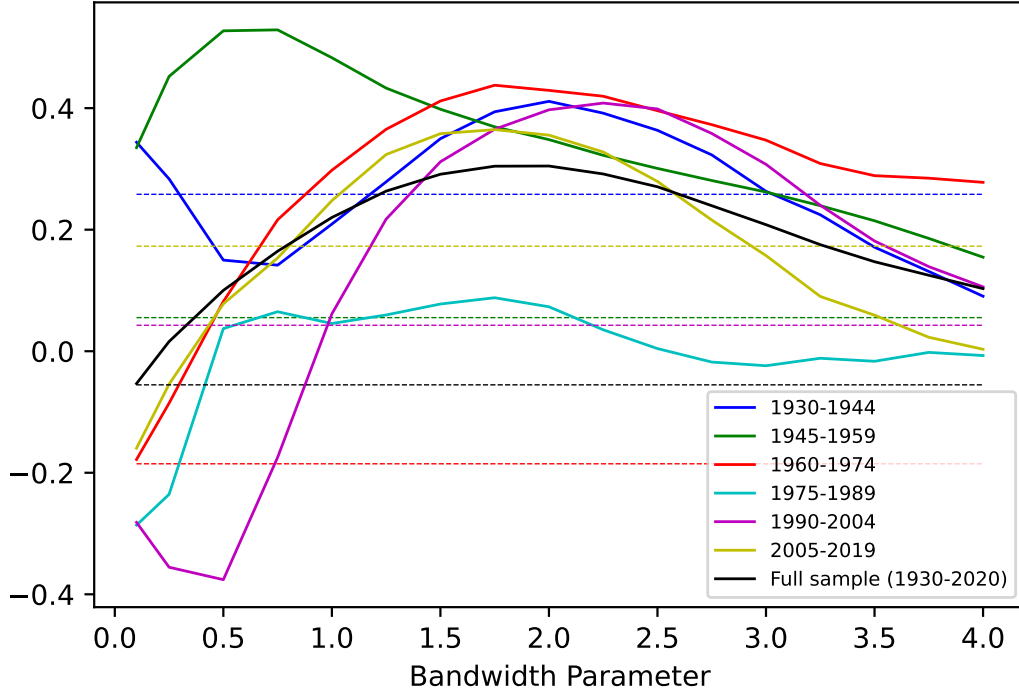


Figure 5: Sharpe ratio sensitivity to periods and bandwidth. We plot average annualized Sharpe ratios obtained on six sub-periods and on the full sample for $p = 600$ RFFs, as a function of the bandwidth parameter of the kernel from the Random Fourier Features. The (dashed) horizontal lines display the return of the strategy when the raw features are used instead of RFFs. In this case, $n = 12$ and $p = 15$. For the sake of visibility, we do not plot the return of the strategy when using raw features for the 1975-1989 period (-0.11). The penalization parameter is $z = 0.01$ (mild regularization). Portfolios are averaged over 500 random draws.

RFFs always outperforms the feasible one. Note that this scheme is unfeasible in practice. However, there are periods during which the RFF-based return is dominated by the simpler linear strategy. Therefore, this further underlines some limitations of the more sophisticated approach. With enough regularization, we see that the simpler model reaches an unconditional (full sample) return that is higher than the high-complexity strategy. This is in line with the conclusions of [Shen and Xiu \(2025\)](#).

5 Counterfactual returns

Our most important theoretical result is Proposition 3, which quantifies the loss in performance based on the misalignment between the in-sample loadings and the out-of-sample loadings. In this last section, we thus propose to assess the strategy's return in the hypothetical scenario where the data would not suffer from posterior drift. This will allow us to quantify the loss from Proposition 3. To this end, we generate counterfactual returns using the time series of estimated loadings $\hat{\beta}_t$ obtained by regressing the RFFs onto the real returns

Period	Linear		RFFs (feasible)		RFFs (hindsight)	
	$z = 0.01$	$z = 100$	$z = 0.01$	$z = 100$	$z = 0.01$	$z = 100$
1930-1944	19.22%	5.00 %	5.08%	2.82%	25.16%	6.64%
1945-1959	4.97%	15.28%	23.45%	18.92%	28.90%	23.45%
1960-1974	-15.40%	2.92%	-6.78%	2.31%	6.73%	4.04%
1975-1989	-49.32%	-0.35%	0.84%	0.49%	0.84%	0.81%
1990-2004	3.63%	7.86%	4.37%	3.60%	4.98%	3.68%
2005-2019	21.01%	10.38%	12.11%	6.33%	12.11%	8.69%
Full sample	-5.87%	6.40%	6.51%	5.75%	13.12%	7.89%

Table 1: Strategy returns under different learning schemes. We exhibit the (monthly) returns of the market-timing strategy under three learning schemes. The column “Linear” refers to the strategy of Equation (14) relying on ridge regression directly applied to Goyal et al.’s macro-economic indicators ($p = 15$). The last two columns display the returns based on Random Features ridge regression. The “hindsight” strategy represents the best case scenario, i.e., if the investor is able to choose the bandwidth with knowledge of the future. The “feasible” strategy consists in choosing the bandwidth parameter based on the best value from the previous period. Note that for the first subperiod (1930-1944), we took the average return over the different values of γ . For these last two schemes, we generate $p = 600$ random features and average portfolios over 500 random draws.

r_{t+1} . Formally, the counterfactual returns are sampled as follows:

$$r_{t+1}^{(c)} = \sum_{k=1}^p \hat{\beta}_t^{(k)} x_t^{(k)} \quad (15)$$

where the $x_t^{(p)}$ are all p predictors (i.e., the RFFs, not the original signals). We underline that this assumes no misspecification as well, i.e., $\theta = 0$ in Equation (1). We opt for simplicity and adding misspecification would artificially burden the exercise with an additional source of errors. Moreover, this route is already explored in Kelly et al. (2024), whereas we focus here on posterior drift.

Once they are generated, the hypothetical returns have low average returns as well as low volatility over the whole period (90 years). This was expected because the ridgeless algorithm selects the solution with the smallest norm. Therefore, we scale these returns in order to match the first two empirical moments of the historical realized returns, i.e.,

$$\tilde{r}_{t+1}^{(c)} = \left(\frac{r_{t+1}^{(c)} - \bar{r}_c}{\sigma_c} \right) \sigma + \bar{r} \quad (16)$$

where \bar{r}_c (resp. \bar{r}) is the sample mean of the counterfactual (resp. realized) returns and σ_c (resp. σ) is their sample standard deviation.

The average returns are plotted in Figure 6 and confirm the theoretical results of Section 2.2. The performance of the strategy is substantially stronger without posterior drift (dashed lines). This difference shown for $z = 0.01$ is more pronounced when the bandwidth is small. As the latter increases, all returns slowly shrink to zero. The case of strong regularization ($z = 100$) corroborate these patterns and is postponed to Figure 11 in the Appendix. Overall, it is clear that when the loadings do not change, the model that is learned allows to generate substantial profits. But when the DGP changes (via the posterior drift), then returns are curtailed.

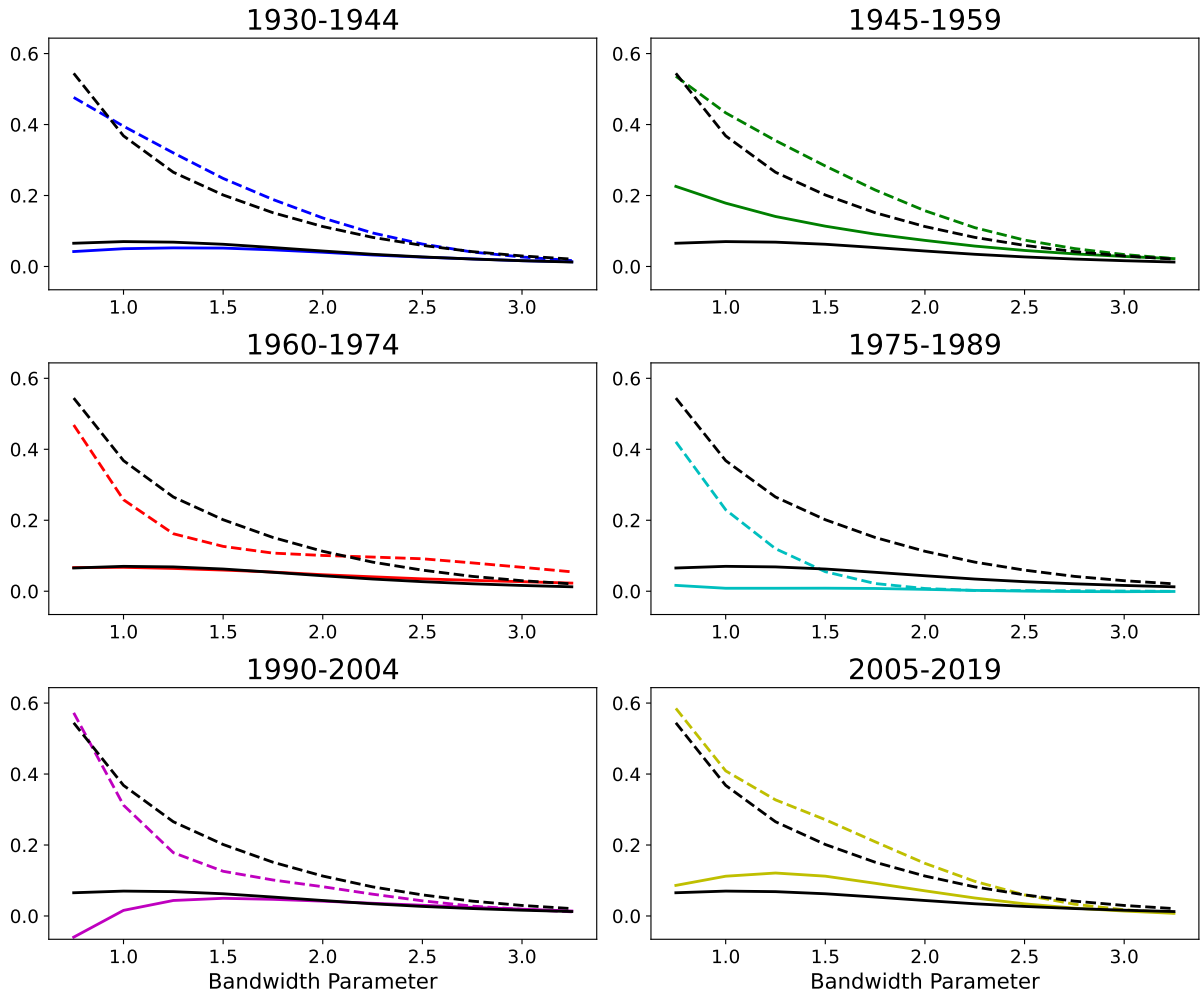


Figure 6: Strategy returns without posterior drift under mild regularization. We plot the real (with posterior drift, solid lines) and the counterfactual (without posterior drift, dashed lines) returns of the strategy obtained on six sub-periods for $p = 600$ RFFs, as a function of the bandwidth parameter of the kernel from the Random Fourier Features. Colored lines represent the strategy returns for the corresponding sub-periods, while **black lines** show returns over the full sample. The penalization parameter is $z = 0.01$ (mild regularization). Returns are averaged over 500 random draws of RFFs.

6 Conclusion

This article seeks to document the sensitivity of the accuracy of overparametrized linear models in equity premium prediction. We find that the results can be promising, but also unstable. They depend on market conditions, even on long horizons, and on a critical parameter that is not straightforward to tune. We attribute these limitations to changes in links between premia and macro variables. These changes strongly attenuate the signal contained in predictors. In sum, large models *can* bring value, but not unconditionally, and one should resort to them while keeping these caveats in mind.

Replication package

The python code to replicate Figures 2 and 3 is available [here](#).

The python code to replicate Figures 4, 5, 6 and 11 is available [here](#).

The python code to replicate Figures 1, 7, 8 and 9 is available [here](#).

The python code to replicate Figure 10 is available [here](#).

References

- Aminikhanghahi, S. and D. J. Cook (2017). A survey of methods for time series change point detection. *Knowledge and Information Systems* 51(2), 339–367.
- Arlot, S., A. Celisse, and Z. Harchaoui (2019). A kernel multiple change-point algorithm via model selection. *Journal of Machine Learning Research* 20(162), 1–56.
- Bai, Z.-D. and Y.-Q. Yin (2008). Limit of the smallest eigenvalue of a large dimensional sample covariance matrix. In *Advances In Statistics*, pp. 108–127. World Scientific.
- Bakalli, G., S. Guerrier, and O. Scaillet (2023). A penalized two-pass regression to predict stock returns with time-varying risk premia. *Journal of Econometrics* 237(2), 105375.
- Bartlett, P. L., P. M. Long, G. Lugosi, and A. Tsigler (2020). Benign overfitting in linear regression. *Proceedings of the National Academy of Sciences* 117(48), 30063–30070.
- Berk, J. (2023). Comment on ‘The Virtue of Complexity in Return Prediction’. *SSRN Working Paper* 4410125.
- Bollerslev, T., J. Li, and Y. Ren (2024). Optimal inference for spot regressions. *American Economic Review* 114(3), 678–708.
- Buncic, D. (2025). Simplified: A closer look at the virtue of complexity in return prediction. *SSRN Working Paper* 5239006.
- Cartea, Á., Q. Jin, and Y. Shi (2025). The limited virtue of complexity in a noisy world. *Available at SSRN*.
- Cheng, C. and A. Montanari (2022). Dimension free ridge regression. *arXiv preprint arXiv:2210.08571*.

- Coulombe, P. G. (2023). Time-varying parameters as ridge regressions. *arXiv Preprint* (2009.00401).
- Dangl, T. and M. Halling (2012). Predictive regressions with time-varying coefficients. *Journal of Financial Economics* 106(1), 157–181.
- Defilippis, L., B. Loureiro, and T. Misiakiewicz (2024). Dimension-free deterministic equivalents for random feature regression. *arXiv preprint arXiv:2405.15699*.
- Enikeeva, F. and Z. Harchaoui (2019). High-dimensional change-point detection under sparse alternatives. *Annals of Statistics* 47(4), 2051–2079.
- Fallahgoul, H. (2025). High-dimensional learning in finance. *SSRN Working Paper* 5281959.
- Farmer, L. E., L. Schmidt, and A. Timmermann (2023). Pockets of predictability. *Journal of Finance* 78(3), 1279–1341.
- Frick, K., A. Munk, and H. Sieling (2014, 05). Multiscale Change Point Inference. *Journal of the Royal Statistical Society Series B: Statistical Methodology* 76(3), 495–580.
- Gagliardini, P., E. Ossola, and O. Scaillet (2016). Time-varying risk premium in large cross-sectional equity data sets. *Econometrica* 84(3), 985–1046.
- Gama, J., I. Žliobaitė, A. Bifet, M. Pechenizkiy, and A. Bouchachia (2014). A survey on concept drift adaptation. *ACM Computing Surveys* 46(4), 1–37.
- Garreau, D. and S. Arlot (2018). Consistent change-point detection with kernels. *Electronic Journal of Statistics* 12(2), 4440–4486.
- Ghysels, E. (1998). On stable factor structures in the pricing of risk: do time-varying betas help or hurt? *Journal of Finance* 53(2), 549–573.
- Goyal, A., I. Welch, and A. Zafirov (2024). A comprehensive 2022 look at the empirical performance of equity premium prediction. *Review of Financial Studies* Forthcoming.
- Hastie, T., A. Montanari, S. Rosset, and R. J. Tibshirani (2020). Surprises in high-dimensional ridgeless least squares interpolation. *arXiv Preprint* (1903.08560).
- Hastie, T., A. Montanari, S. Rosset, and R. J. Tibshirani (2022). Surprises in high-dimensional ridgeless least squares interpolation. *Annals of Statistics* 50(2), 949–986.
- Hu, X. and Z. Lin (2025). Transfer learning meets functional linear regression: No negative transfer under posterior drift. In *Proceedings of the AAAI Conference on Artificial Intelligence*, Volume 39, pp. 17351–17358.
- Kelly, B. T., S. Malamud, and K. Zhou (2024). The virtue of complexity in return prediction. *Journal of Finance* 79(1), 459–503.
- Knowles, A. and J. Yin (2017). Anisotropic local laws for random matrices. *Probability Theory and Related Fields* 169, 257–352.
- Londschien, M., P. Bühlmann, and S. Kovács (2023). Random forests for change point detection. *Journal of Machine Learning Research* 24(216), 1–45.

- Lu, J., A. Liu, F. Dong, F. Gu, J. Gama, and G. Zhang (2018). Learning under concept drift: A review. *IEEE Transactions on Knowledge and Data Engineering* 31(12), 2346–2363.
- Lung-Yut-Fong, A., C. Lévy-Leduc, and O. Cappé (2015). Homogeneity and change-point detection tests for multivariate data using rank statistics. *Journal de la Société Française de Statistique* 156(4), 133–162.
- Maity, S., D. Dutta, J. Terhorst, Y. Sun, and M. Banerjee (2024). A linear adjustment-based approach to posterior drift in transfer learning. *Biometrika* 111(1), 31–50.
- Misiakiewicz, T. and A. Montanari (2023). Six lectures on linearized neural networks. *arXiv preprint arXiv:2308.13431*.
- Misiakiewicz, T. and B. Saeed (2024). A non-asymptotic theory of kernel ridge regression: deterministic equivalents, test error, and gcv estimator. *arXiv preprint arXiv:2403.08938*.
- Nagel, S. (2025). Seemingly virtuous complexity in return prediction. *Working Paper*.
- Pav, S. E. (2021). *The Sharpe Ratio: Statistics and Applications*. Chapman and Hall/CRC.
- Power, A., Y. Burda, H. Edwards, I. Babuschkin, and V. Misra (2022). Grokking: Generalization beyond overfitting on small algorithmic datasets. *arXiv Preprint (2201.02177)*.
- Roy, S., Y. Atchadé, and G. Michailidis (2016, 09). Change Point Estimation in High Dimensional Markov Random-Field Models. *Journal of the Royal Statistical Society Series B: Statistical Methodology* 79(4), 1187–1206.
- Shen, Z. and D. Xiu (2025). Can machines learn weak signals? *SSRN Working Paper 4748784*.
- Silverstein, J. W. (1995). Strong convergence of the empirical distribution of eigenvalues of large dimensional random matrices. *Journal of Multivariate Analysis* 55(2), 331–339.
- Varma, V., R. Shah, Z. Kenton, J. Kramár, and R. Kumar (2023). Explaining grokking through circuit efficiency. *arXiv Preprint (2309.02390)*.
- Wang, B. and X. Qiao (2025). Conformal prediction under generalized covariate shift with posterior drift. *arXiv Preprint 2502.17744*.
- Welch, I. and A. Goyal (2008). A comprehensive look at the empirical performance of equity premium prediction. *Review of Financial Studies* 21(4), 1455–1508.
- Yin, Y.-Q., Z.-D. Bai, and P. R. Krishnaiah (1988). On the limit of the largest eigenvalue of the large dimensional sample covariance matrix. *Probability theory and related fields* 78, 509–521.

A Appendix

A.1 Simulated returns under strong regularization (equidistributed parameters vectors)

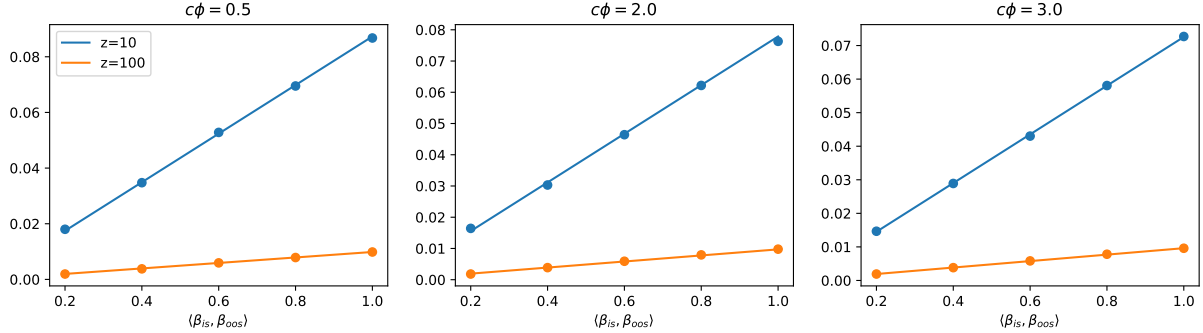


Figure 7: Simulated and theoretical returns of the strategy under strong regularization. The model's true complexity is $c = 3$ ($p + q = 300$, $n = 100$). z is the regularization parameter of the ridge estimator. We plot the theoretical returns of the strategy as per Proposition 3 (solid line). Simulated returns (dots) are generated according to the process described in Section 3 and are averaged over 100,000 random draws.

A.2 Simulated returns (concentrated parameters vectors)

We simulate the expected return of the market timing strategy following the process described in Section 3 except for the true parameters vectors related to the observed data, β_{is} and β_{00s} .

In this section, the latter are concentrated on some directions of Σ . The first half of the coefficients of β_{is} are equal to 1. The remaining components are equal to 0.1. Furthermore, we normalize β_{is} so it has unit signal, i.e. $\|\beta_{is}\|^2 = 1$.

We consider a sequence of $(\beta_{00s,k})_k$, $k \in \{1, 2, 3, 4, 5\}$, with unit signal. To this end, let the first $(50/k)\%$ of the coefficients of $\beta_{00s,k}$ be equal to 1 while the remaining components are set to 0.1. As for β_{is} , we normalize these vectors so they have unit signal, namely $\|\beta_{00s,k}\|^2 = 1$ for any $k \in \{1, 2, 3, 4, 5\}$.

We analogously generate the true parameters vectors for the unobserved data, θ_{is} and θ_{00s} , setting only a different number of coefficients, viz. q instead of p .

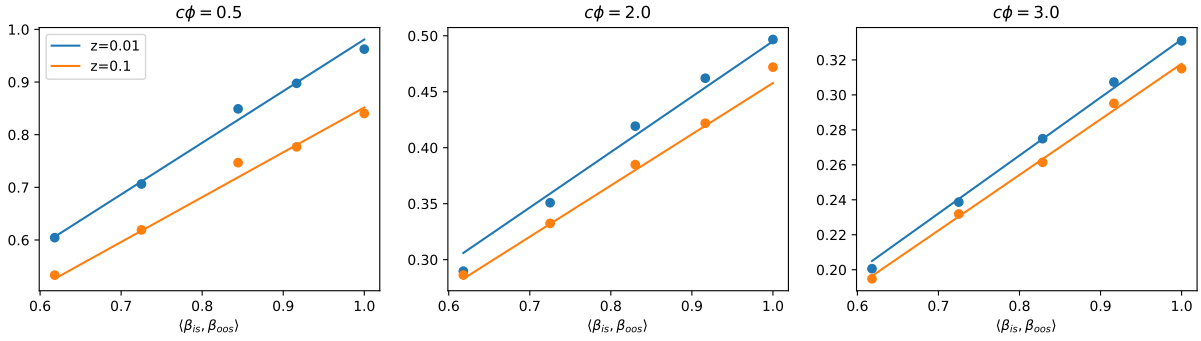


Figure 8: Simulated and theoretical returns of the strategy under mild regularization (concentrated (true) parameters vectors). The model's true complexity is $c = 3$ ($p + q = 300, n = 100$). z is the regularization parameter of the ridge estimator. We plot the theoretical returns of the strategy as per Proposition 3 (solid line). Simulated returns (dots) are generated according to the process described in Section A.2 and are averaged over 100,000 random draws.

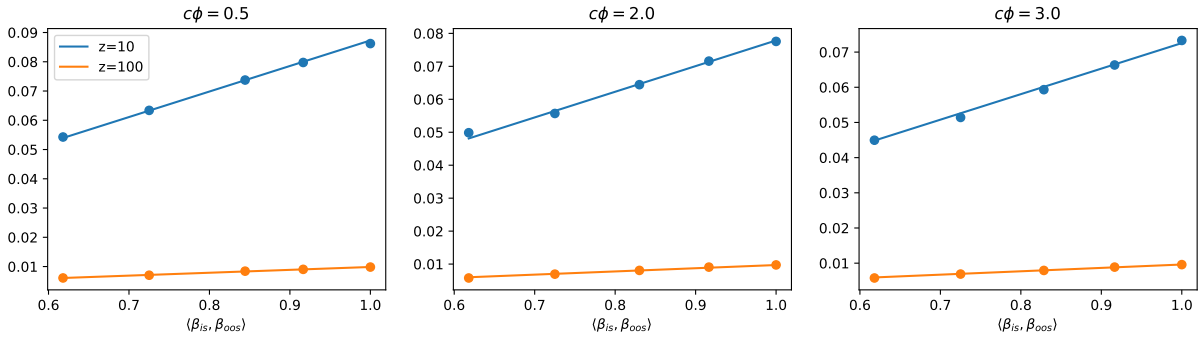


Figure 9: Simulated and theoretical returns of the strategy under strong regularization (concentrated (true) parameters vectors). The model's true complexity is $c = 3$ ($p + q = 300, n = 100$). z is the regularization parameter of the ridge estimator. We plot the theoretical returns of the strategy as per Proposition 3 (solid line). Simulated returns (dots) are generated according to the process described in Section A.2 and are averaged over 100,000 random draws.

The convergence of average simulated returns towards theoretical returns is illustrated in Figure 10. Note that returns are averaged over 10 million random draws which is already computationally prohibitive when $n > 100$. High precision (errors below 0.2%) is already reached for $n = 130$. According to Propositions 4 and 8, the gaps tend to zero as the number of samples, n , increases. Better convergence patterns (strictly decreasing graphically) could also be obtained by averaging over a more substantial number of draws, but at the cost of extended computational times.

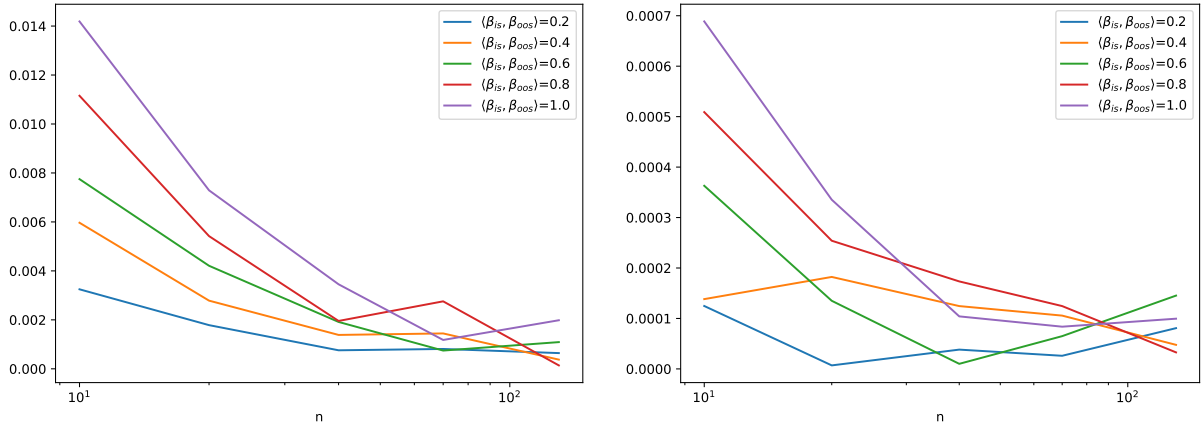


Figure 10: Convergence of average simulated returns. We plot the difference between theoretical and average simulated returns. The true model’s complexity is $c = 3$ while the working model has a complexity of $c\phi = 0.5$. The left plot shows the case when the penalization parameter is $z = 0.1$ (mild regularization), while the right one pertains to $z = 10$ (strong regularization). Simulated returns are generated according to the process described in Section 3 and are averaged over 10 million random draws.

A.3 Counterfactual returns with strong regularization

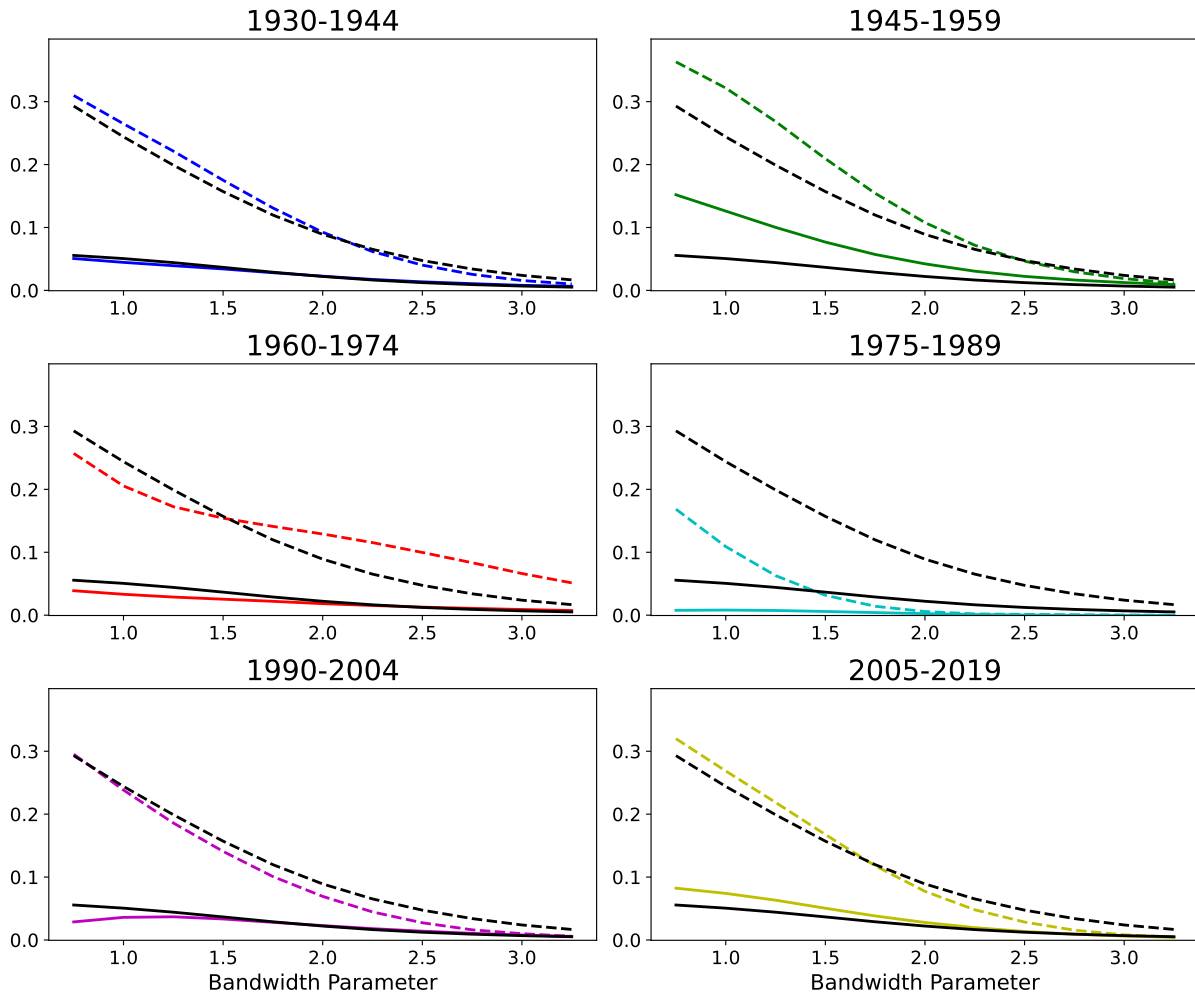


Figure 11: Portfolio returns without concept drift under strong regularization. We plot the real (with concept drift, solid lines) and the counterfactual (without concept drift, dashed lines) returns of the strategy obtained on six sub-periods for $P = 600$ RFFs, as a function of the bandwidth parameter of the kernel from the Random Fourier Features. Colored lines represent the strategy returns for the corresponding sub-periods, while **black lines** show returns over the full sample. The penalization parameter is $z = 100$ (strong regularization). Returns are averaged over 500 random draws of RFFs.

A.4 Proof of Proposition 1

A.4.1 Preliminary results and discussions

We start with a few useful results that correspond to the correctly specified model ($\theta = 0$) in the isotropic case $\Sigma = I$. This will give us building blocks for subsequent calculations.

Lemma 1. *The estimator β_{is} in (3) has out-of-sample bias and variance (defined in Equation (2)):*

$$B_X(\hat{\beta}_{\text{is}}, \beta_{\text{OOS}}) = \beta_{\text{is}}' \Pi \Sigma \Pi \beta_{\text{is}} + (\beta_{\text{OOS}} - \beta_{\text{is}})' \Sigma (\beta_{\text{OOS}} - \beta_{\text{is}}) + 2(\beta_{\text{OOS}} - \beta_{\text{is}})' \Sigma \Pi \beta_{\text{is}} \quad (17)$$

$$V_X(\hat{\beta}_{\text{is}}, \beta_{\text{OOS}}) = n^{-1} \sigma^2 \text{Tr}(\hat{\Sigma}^+ \Sigma), \quad (18)$$

where $\Pi = I - \hat{\Sigma}^+ \hat{\Sigma}$, I being the identity matrix.

This can be proven as in [Hastie et al. \(2022\)](#), notably by plugging $\mathbb{E}[\hat{\beta}_u | X] = \hat{\Sigma}^+ \hat{\Sigma} \beta_u$ into Equation (2). Compared to the i.i.d. case in which β remains the same for both samples, only the bias is changed and has new additional terms that reflect the drift between β_{is} and β_{OOS} . Asymptotically, as both dimensions increase to infinity such that $p/n \rightarrow \gamma \in (0, 1)$, it will hold that $\Pi = 0$ as long as all eigenvalues are bounded from below by some strictly positive constant. Thus, compared to Proposition 2 in [Hastie et al. \(2022\)](#), it holds that

$$\lim_{n,p \rightarrow \infty} R_X(\hat{\beta}_{\text{is}}, \beta_{\text{OOS}}) = \sigma^2 \frac{\gamma}{1 - \gamma} + \|\beta_{\text{OOS}} - \beta_{\text{is}}\|_{\Sigma}^2, \quad p/n \rightarrow \gamma \in (0, 1). \quad (19)$$

Hence, we clearly see that in contrast with the case when β does not change, there is an additional term that pertains to the change between the training loadings (β_{is}) and the testing ones (β_{OOS}). This quantity is strictly positive if Σ is positive definite and it increases with each element-wise absolute distance $|\beta_{\text{is},p} - \beta_{\text{OOS},p}|$ when correlations are positive, or when Σ is diagonally dominant.

We next turn the overparametrized regime in which the number of predictors lies asymptotically *above* the number of observations, i.e., $\gamma > 1$. This case is much more involved and for simplicity, we will only tackle it in the simplified framework in which predictors are independent (and have common variance), i.e., when $\Sigma = I$ - this is commonly referred to as the *isotropic* feature case.

In this particular case, the variance term is the same as in the original article, that is, $V_X(\hat{\beta}_{\text{is}}, \beta_{\text{OOS}}) = \sigma^2(\gamma - 1)^{-1}$. However, the bias term is directly impacted and, in addition to the original term $\|\beta_{\text{is}}\|_2^2(1 - \gamma^{-1})$, there are two quantities, namely $\|\beta_{\text{is}} - \beta_{\text{OOS}}\|_2^2$ and $2(\beta_{\text{OOS}} - \beta_{\text{is}})' \Pi \beta_{\text{is}} \rightarrow 2(1 - \gamma^{-1})(\beta_{\text{OOS}} - \beta_{\text{is}})' \beta_{\text{is}}$. The first one is obvious from the second term of the bias in Lemma 1 when $\Sigma = I$. The second limiting value can be determined exactly as in the proof of Theorem 1 in [Hastie et al. \(2022\)](#). Adding all three terms gives

$$\lim_{n,p \rightarrow \infty} R_X(\hat{\beta}_{\text{is}}, \beta_{\text{OOS}}) = \sigma^2(\gamma - 1)^{-1} + \gamma^{-1} \|\beta_{\text{is}}\|_2^2 + \|\beta_{\text{OOS}}\|_2^2 - 2\gamma^{-1} \beta_{\text{OOS}}' \beta_{\text{is}} \quad (20)$$

$$= \sigma^2(\gamma - 1)^{-1} + \gamma^{-1} \|\beta_{\text{is}} - \beta_{\text{OOS}}\|_2^2 + (1 - \gamma^{-1}) \|\beta_{\text{OOS}}\|_2^2, \quad (21)$$

where in the second equation all terms are positive. In particular, it is clear that the risk increases with $|\beta_{\text{is},p} - \beta_{\text{OOS},p}|$ which measures the absolute change in the p^{th} loading of the model. Intuitively, the more the data generating process changes, the larger the out-of-sample error. The general case involves the empirical distribution of the eigenvalues of Σ and is out of the scope of the present paper, but it can be conjectured that the limiting risk will also involve the change term $\Delta = \beta_{\text{is}} - \beta_{\text{OOS}}$.

A.4.2 The proof

Let (x_0, w_0) be a random draw of $P_{x,w}$ that is independent from the training data.

$$\begin{aligned}
R_X^m(\hat{\beta}_{\text{is}}, \beta_{\text{oos}}, \theta) &= \mathbb{E}[(x_0 \hat{\beta}_{\text{is}} - \mathbb{E}[y_0|x_0, w_0])^2|X] \\
&= \mathbb{E}[(x_0 \hat{\beta}_{\text{is}} - \mathbb{E}[y_0|x_0] + \mathbb{E}[y_0|x_0] - \mathbb{E}[y_0|x_0, w_0])^2|X] \\
&= \mathbb{E}[(x_0 \hat{\beta}_{\text{is}} - \mathbb{E}[y_0|x_0])^2|X] + \mathbb{E}[(\mathbb{E}[y_0|x_0] - \mathbb{E}[y_0|x_0, w_0])^2] \\
&\quad + 2\mathbb{E}[(x_0 \hat{\beta}_{\text{is}} - \mathbb{E}[y_0|x_0])(\mathbb{E}[y_0|x_0] - \mathbb{E}[y_0|x_0, w_0])|X]
\end{aligned}$$

In addition, we have $\mathbb{E}[y_0|x_0] = x_0' \beta_{\text{oos}} + \mathbb{E}[w_0' \theta_{\text{oos}}|x_0]$ and $\mathbb{E}[y_0|x_0, w_0] = x_0' \beta_{\text{oos}} + w_0' \theta$. Focusing on the cross-term, note that by the law of iterated expectations we have

$$\begin{aligned}
&\mathbb{E}[(x_0 \hat{\beta}_{\text{is}} - \mathbb{E}[y_0|x_0])(\mathbb{E}[y_0|x_0] - \mathbb{E}[y_0|x_0, w_0])|X] \\
&= \mathbb{E}[(x_0 \hat{\beta}_{\text{is}} - x_0' \beta_{\text{oos}} - \mathbb{E}[w_0' \theta_{\text{oos}}|x_0])(\mathbb{E}[w_0' \theta_{\text{oos}}|x_0] - w_0' \theta_{\text{oos}})|X] \\
&= \mathbb{E}\left[\mathbb{E}[(x_0 \hat{\beta}_{\text{is}} - x_0' \beta_{\text{oos}} - \mathbb{E}[w_0' \theta_{\text{oos}}|x_0])(\mathbb{E}[w_0' \theta_{\text{oos}}|x_0] - w_0' \theta_{\text{oos}})|x_0, X] \middle| X\right] \\
&= \mathbb{E}\left[(x_0 \hat{\beta}_{\text{is}} - x_0' \beta_{\text{oos}} - \mathbb{E}[w_0' \theta_{\text{oos}}|x_0])(\mathbb{E}[w_0' \theta_{\text{oos}}|x_0] - \mathbb{E}[w_0' \theta_{\text{oos}}|x_0, X]) \middle| X\right]
\end{aligned}$$

w_0 is independent from X . Then, $\mathbb{E}[w_0' \theta_{\text{oos}}|x_0, X] = \mathbb{E}[w_0' \theta_{\text{oos}}|x_0]$ and the cross term vanishes. Therefore,

$$R_X^m(\hat{\beta}_{\text{is}}, \beta_{\text{oos}}, \theta) = \mathbb{E}[(x_0'(\hat{\beta}_{\text{is}} - \beta_{\text{oos}}))^2|X] + \mathbb{E}[(w_0' \theta_{\text{oos}} - \mathbb{E}[w_0' \theta_{\text{oos}}|x_0])^2] = R_X(\hat{\beta}_{\text{is}}, \beta_{\text{oos}}) + M(\theta_{\text{oos}})$$

The two cases (under- versus over-parametrized models) are obtained thanks to Equations (19) and (21). In fact, when covariates are i.i.d. with unit variance, the training labels can be thought to have variance $\sigma^2 + \|\theta_{\text{is}}\|_2^2$. Then, it suffices to plug $\sigma^2 \rightarrow \sigma^2 + \|\theta_{\text{is}}\|_2^2$ into (19) or (21) and add the misspecification bias $M(\theta_{\text{oos}}) = \|\theta_{\text{oos}}\|_2^2$ to obtain the desired prediction risk. This completes the proof.

A.5 Expected returns: theoretical results

Let $\lambda_1 \geq \lambda_2 \geq \dots \geq \lambda_p \geq 0$ be the eigenvalues of Σ_x . Denote by δ_{λ_i} a unit mass concentrated at λ_i . Then, the empirical spectral distribution (ESD) of Σ_x is given by

$$\mu \equiv \mu(\lambda) = \frac{1}{p} \sum_{i=1}^p \delta_{\lambda_i} \quad (22)$$

For $i \in \{1, \dots, p\}$, denote by v_i the eigenvector of Σ_x associated with the eigenvalue λ_i . Then, we also define the

$$\begin{aligned}
\zeta_{is} &:= \frac{1}{\|\beta_{is}\|^2} \sum_{i=1}^p |\langle \beta_{is}, v_i \rangle|^2 \delta_{\lambda_i} \\
\zeta_{oos} &:= \frac{1}{\|\beta_{oos}\|^2} \sum_{i=1}^p |\langle \beta_{oos}, v_i \rangle|^2 \delta_{\lambda_i} \\
\zeta_r &:= \begin{cases} \frac{1}{\|\beta_{oos} - \beta_{is}\|^2} \sum_{i=1}^p |\langle \beta_{oos} - \beta_{is}, v_i \rangle|^2 \delta_{\lambda_i} & \beta_{is} \neq \beta_{oos} \\ 0 & \beta_{is} = \beta_{oos} \end{cases}
\end{aligned} \tag{23}$$

where the subscript r in ζ_r stands for "residual". Note that these three quantities are density measures. In particular, they are reweighted counterparts of μ where the summands account for the projections of β_{is} , β_{oos} or the residual vector $\beta_{oos} - \beta_{is}$ on the eigenvectors of Σ_x . These densities are often referred to as the eigenvector empirical spectral distributions (the so-called VESDs) or local densities of the states β_{is} , β_{oos} and $\beta_{oos} - \beta_{is}$, respectively.

Finally, we set

$$\zeta_d \equiv \zeta_d(\lambda) := \frac{1}{\|\beta_{is}\| \|\beta_{oos}\|} \sum_{i=1}^p \langle \beta_{is}, v_i \rangle \langle v_i, \beta_{oos} \rangle \delta_{\lambda_i}, \tag{24}$$

where the subscript d stands for "drift". We make two observations regarding ζ_d . First, it is a signed measure and no longer a density. Second, it can be decomposed as a function of ζ_{is} , ζ_{oos} and ζ_r as follows:

$$\zeta_d = \frac{1}{2\|\beta_{is}\| \|\beta_{oos}\|} \left(\|\beta_{is}\|^2 \zeta_{is} + \|\beta_{oos}\|^2 \zeta_{oos} - \|\beta_{oos} - \beta_{is}\|^2 \zeta_r \right).$$

As is customary in the literature, we will need a few technical assumptions.

Assumption A.1. $\lambda_1 = \|\Sigma_x\|_{\text{op}} \leq \tau^{-1}$.

Assumption A.2. $\mu([0, \tau]) \leq 1 - \tau$.

Condition [A.1](#) and [A.2](#) require the eigenvalues of Σ_x to be bounded and not to be concentrated at zero.⁸

Assumption A.3. μ weakly converges to a density measure ν . Besides, $\text{supp}(\nu) \subseteq [0, \infty)$.

Assumption A.4. ζ_{is} , ζ_{oos} and ζ_r weakly converges to some density measures η_{is} , η_{oos} and η_r respectively. Moreover, these limiting measures have support on $[0, \infty)$.

Finally, the latter two assumptions ensure that the densities defined in [\(22\)](#) and [\(23\)](#) are well-behaved in the asymptotic proportional regime, i.e. when $n, p \rightarrow \infty$ such that $p/n \rightarrow c\phi$.

Remark 3. *Assumption A.4 implies that*

$$\zeta_d = \frac{1}{2\|\beta_{is}\| \|\beta_{oos}\|} \left(\|\beta_{is}\|^2 \zeta_{is} + \|\beta_{oos}\|^2 \zeta_{oos} - \|\beta_{oos} - \beta_{is}\|^2 \zeta_r \right)$$

weakly converges to a (possibly signed) measure η_d .

⁸As noted in [Hastie et al. \(2020\)](#), this assumption could be relaxed by requiring only $d < p$ of the eigenvalues to be non-vanishing and by consequently redefining $c\phi = d/n$. However, we pursue with the stronger hypothesis to avoid cumbersome notations in the statement of the results and proofs.

Next, we define the solutions to two different equations, $m_n(z; c\phi, \mu)$ and $s_0(c\phi, \mu)$, that will appear in the subsequent theoretical results. Denote by \mathbb{C}_+ the complex upper half plane, i.e. $\mathbb{C}_+ = \{z \in \mathbb{C} : \Im(z) > 0\}$.

Definition 4. Let $c\phi = p/n > 0$ and $z \in \mathbb{C}_+$. Define $m_n := m_n(z; c\phi, \mu)$ as the unique solution in \mathbb{C}_+ to

$$m_n = \int \frac{1}{\lambda(1 - c\phi - c\phi z m_n) - z} d\mu(\lambda).$$

This definition is extended to $\Im(z) = 0$ whenever possible.

Definition 5. Let $s_0 := s_0(c\phi, \mu)$ be the unique non-negative solution to

$$1 - \frac{1}{c\phi} = \int \frac{1}{1 + \lambda c\phi s_0} d\mu(\lambda).$$

Lastly, we define the following quantity which repeatedly appear in the different characterizations of the expected return of the strategy. Note that it does not depend on the regularization parameter, z .

Definition 6.

$$\begin{aligned} \bar{H}_n(\zeta_d) &= \langle \beta_{oos}, \beta_{is} \rangle_{\Sigma} \\ &= \|\beta_{is}\| \|\beta_{oos}\| \int \lambda d\zeta_d(\lambda). \end{aligned}$$

A.5.1 Well-specified model and ridge regularization

Here, we consider that the true model is known. Hence, throughout this subsection, $\theta = 0$ and consequently, $q = 0$, $\phi = 1$ and $\Sigma \equiv \Sigma_x$.

Let

$$F_n(z) = -z \langle \beta_{oos}, \Sigma(\hat{\Sigma} + zI)^{-1} \beta_{is} \rangle,$$

and define:

$$\begin{aligned} \bar{F}_n(z; \mu, \zeta_d) &= -z \langle \beta_{oos}, \Sigma(zI + (czm_n(-z; c, \mu) + 1 - c)\Sigma)^{-1} \beta_{is} \rangle \\ &= -z \|\beta_{is}\| \|\beta_{oos}\| \int \frac{\lambda}{\lambda(czm_n(-z; c, \mu) + 1 - c) + z} d\zeta_d(\lambda) \end{aligned}$$

where $m_n := m_n(-z; c, \mu)$ is given in Definition 4.

Moreover, consider the following hypothesis.

Assumption A.5. The covariates have the form $x_i = \Sigma^{1/2} z_i$ with $z_i = (z_{i1}, z_{i2}, \dots, z_{ip})$ having independent entries. In addition, for all $j \in \{1, \dots, p\}$, $\mathbb{E}[z_{ij}] = 0$, $\mathbb{E}[z_{ij}^2] = 1$ and $\mathbb{E}[|z_{ij}|^k] \leq C_k < \infty$ for all $k \geq 2$.

We now state a number of lemmas that will be useful in the remainder of the proofs. In particular, Lemma 2 establishes non-asymptotic bounds for the gap between F_n and \bar{F}_n which implies almost sure convergence as proved in Lemma 4.

Lemma 2. Let $n^{-2/3+\tau} \leq z \leq \tau^{-1}$ and Assumptions (2.2), (A.1), (A.2) and (A.5) hold. Then, for any $D > 0$ and $\varepsilon > 0$, there exist $n_0 := n_0(\varepsilon, D)$ such that for $n \geq n_0$,

$$|F_n(z) - \bar{F}_n(z; \mu, \zeta_d)| \leq \frac{\|\Sigma\beta_{oos}\| \|\beta_{is}\|}{n^{\frac{1}{2}-\varepsilon} z} \quad (25)$$

holds with probability $1 - n^{-D}$.

Proof. The proof mainly consists in an application of the anisotropic local law derived by Knowles and Yin (2017).

First, let $\tilde{\beta}_{(oos, \Sigma)} = (\Sigma\beta_{oos})/\|\Sigma\beta_{oos}\| = (\Sigma\beta_{oos})/\|\beta_{oos}\|_\Sigma$ and $\tilde{\beta}_{is} = \beta_{is}/\|\beta_{is}\|$. Furthermore, define

$$\begin{aligned} J_n(z) &= -z \langle \tilde{\beta}_{(oos, \Sigma)}, (\hat{\Sigma} + zI)^{-1} \tilde{\beta}_{is} \rangle \\ \bar{J}_n(z; \mu, \zeta_d) &= -z \langle \tilde{\beta}_{(oos, \Sigma)}, (zI + (czm_n(-z; c, \mu) + 1 - c)\Sigma)^{-1} \tilde{\beta}_{is} \rangle, \end{aligned}$$

which are standardized counterparts of F_n and \bar{F}_n .

Define $\mathbf{D}(\tau, n) = \{z \in \mathbb{C}_+ : |z| \geq \tau, |\Re(z)| \leq \tau^{-1}, 0 \leq \Im(z) \leq \tau^{-1}\}$ and $\mathbf{D}^O(\tau, n) = \{z \in \mathbf{D}(\tau, n) : \Re(z) \leq -n^{-2/3+\tau}\}$. For the sake of simplicity, we drop the dependence on τ and n and let $\mathbf{D}^O := \mathbf{D}^O(\tau, n)$.

Consider $z \in \mathbb{C}_-$, i.e. $\Im(z) < 0$, such that $\Re(z) \geq n^{-2/3+\tau}$. Hence, $-z \in \mathbf{D}^O$. Then, as per Theorem 3.16. (i) and Remark 3.17. in Knowles and Yin (2017), for any $D > 0$ and $\varepsilon > 0$, there exist $n_0 := n_0(\varepsilon, D)$ such that for $n \geq n_0$, the following holds with probability $1 - n^{-D}$

$$|J_n(z) + \langle \tilde{\beta}_{(oos, \Sigma)}, (I + r_n(-z)\Sigma)^{-1} \tilde{\beta}_{is} \rangle| \leq n^\varepsilon \sqrt{\frac{\Im(r_n(-z))}{n\Im(-z)}},$$

with $r_n = r_n(-z)$ the unique solution in \mathbb{C}_+ of the equation

$$\frac{1}{r_n} = -z + c \int \frac{\lambda}{1 + r_n \lambda} d\mu(\lambda), \quad \Im(-z) > 0.$$

where $\lambda_1 \geq \lambda_2 \geq \dots \geq \lambda_p \geq 0$ are the eigenvalues of Σ .

Moreover, $r_n(-z)$ is the Stieltjes transform of a probability measure ρ_n with bounded support in $[0, \infty)$.

Therefore, we have

$$\Im(r_n(-z)) = \Im\left(\int \frac{1}{x+z} d\rho_n(x)\right) = \int \frac{-\Im(z)}{(x + \Re(z))^2 + \Im(z)^2} d\rho_n(x).$$

This implies

$$|\Im(r_n(-z))| \leq \frac{|\Im(z)|}{\Re(z)^2}.$$

and consequently,

$$|J_n(z) + \langle \tilde{\beta}_{(oos, \Sigma)}, (I + r_n(-z)\Sigma)^{-1} \tilde{\beta}_{is} \rangle| \leq \frac{1}{n^{1/2-\varepsilon} \Re(z)} \sqrt{\frac{|\Im(z)|}{\Im(-z)}}.$$

Note that r_n is the companion Stieltjes transform of the ESD defined in (22). However, we would like to relate the deterministic equivalent of $J_n(z)$ to the eigenvalue distribution of the covariance matrix, or equivalently to its Stieltjes transform. This is possible thanks to the following (well-known) relation in random matrix theory (see e.g. [Silverstein \(1995\)](#))

$$r_n(-z) = cm_n(-z; c, \mu) + \frac{1-c}{z}. \quad (26)$$

Here, $m_n := m_n(-z; c, \mu)$ is the unique solution in \mathbb{C}_+ to

$$m_n = \int \frac{1}{\lambda(1-c + czm_n) + z} d\mu(\lambda), \quad \Im(-z) > 0.$$

Replacing $r_n(-z)$ as per Equation (26) in $-\langle \tilde{\beta}_{(oos, \Sigma)}, (I + r_n(-z)\Sigma)^{-1} \tilde{\beta}_{is} \rangle$, we obtain

$$|J_n(z) - \bar{J}_n(z; \mu, \zeta_d)| \leq \frac{1}{n^{1/2-\varepsilon} \Re(z)} \sqrt{\frac{|\Im(z)|}{\Im(-z)}}.$$

Taking $\Im(z) \rightarrow 0$, we get the following inequality with probability $1 - n^{-D}$:

$$|J_n(z) - \bar{J}_n(z; \mu, \zeta_d)| \leq \frac{1}{n^{1/2-\varepsilon} z}, \quad z \in [n^{-2/3+\tau}, \tau^{-1}],$$

for any sufficiently large n .

Finally, multiplying both sides of the inequality by $\|\Sigma\beta_{oos}\| \|\beta_{is}\|$, we obtain (41).

The proof of Lemma 2 is complete. □

Lemma 3. ([Yin et al. \(1988\)](#), [Bai and Yin \(2008\)](#)) Let Y be a $n \times p$ matrix with i.i.d. entries, $(y_{ij})_{1 \leq i \leq n, 1 \leq j \leq p}$. Besides, for all i, j , $\mathbb{E}[y_{ij}] = 0$, $\mathbb{E}[y_{ij}^2] = 1$ and $\mathbb{E}[|y_{ij}|^{4+a}] \leq C < \infty$ for $a > 0$. Then, in the limit, as $p, n \rightarrow \infty$, $p/n \rightarrow c \in (0, \infty)$,

$$\limsup \lambda_{\max} \left(\frac{1}{n} Y'Y - (1+c)I \right) \leq 2\sqrt{c}, \quad a.s.$$

Lemma 4. Let $z > \tau$ and Assumptions (2.1), (2.2), (A.1), (A.2), (A.3), (A.4) hold. Then

$$F_n(z) \xrightarrow{a.s.} \bar{F}_n(z; \nu, \eta_d)$$

Proof. Rewrite $F_n(z; \hat{\Sigma}, \Sigma) = F_n(z)$ to highlight the dependence of the function on the sample covariance, $\hat{\Sigma}$, and the population covariance, Σ .

Note that

$$\begin{aligned} |F_n(z; \hat{\Sigma}, \Sigma_1) - F_n(z; \hat{\Sigma}, \Sigma_2)| &\leq z \|\beta_{is}\| \|\beta_{oos}\| \|(\hat{\Sigma} + zI)^{-1}\|_{\text{op}} \|\Sigma_1 - \Sigma_2\|_{\text{op}} \\ &\leq \|\beta_{is}\| \|\beta_{oos}\| \|\Sigma_1 - \Sigma_2\|_{\text{op}} \end{aligned}$$

The second inequality follows after observing that $\|(\hat{\Sigma} + zI)^{-1}\|_{\text{op}} \leq z^{-1}$.

We also have

$$\begin{aligned}
|F_n(z; \hat{\Sigma}_1, \Sigma) - F_n(z; \hat{\Sigma}_2, \Sigma)| &\leq z \|\beta_{is}\| \|\beta_{oos}\| \|\Sigma\|_{\text{op}} \|(\hat{\Sigma}_1 + zI)^{-1} - (\hat{\Sigma}_2 + zI)^{-1}\|_{\text{op}} \\
&\leq z\tau^{-1} \|\beta_{is}\| \|\beta_{oos}\| \|(\hat{\Sigma}_1 + zI)^{-1}(\hat{\Sigma}_1 + zI - (\hat{\Sigma}_2 + zI))(\hat{\Sigma}_2 + zI)^{-1}\|_{\text{op}} \\
&\leq z\tau^{-1} \|\beta_{is}\| \|\beta_{oos}\| \|(\hat{\Sigma}_1 - \hat{\Sigma}_2)\|_{\text{op}} \|(\hat{\Sigma}_1 + zI)^{-1}\|_{\text{op}} \|(\hat{\Sigma}_2 + zI)^{-1}\|_{\text{op}} \\
&\leq z^{-1}\tau^{-1} \|\beta_{is}\| \|\beta_{oos}\| \|(\hat{\Sigma}_1 - \hat{\Sigma}_2)\|_{\text{op}} \\
&\leq \tau^{-2} \|\beta_{is}\| \|\beta_{oos}\| \|(\hat{\Sigma}_1 - \hat{\Sigma}_2)\|_{\text{op}}
\end{aligned}$$

Therefore, setting $C = \max\{\|\beta_{is}\| \|\beta_{oos}\|, \tau^{-2} \|\beta_{is}\| \|\beta_{oos}\|\}$, we have

$$\begin{aligned}
|F_n(z; \hat{\Sigma}_1, \Sigma_1) - F_n(z; \hat{\Sigma}_2, \Sigma_2)| &= |F_n(z; \hat{\Sigma}_1, \Sigma_1) - F_n(z; \hat{\Sigma}_1, \Sigma_2) + F_n(z; \hat{\Sigma}_1, \Sigma_2) - F_n(z; \hat{\Sigma}_2, \Sigma_2)| \\
&\leq |F_n(z; \hat{\Sigma}_1, \Sigma_1) - F_n(z; \hat{\Sigma}_1, \Sigma_2)| + |F_n(z; \hat{\Sigma}_1, \Sigma_2) - F_n(z; \hat{\Sigma}_2, \Sigma_2)| \\
&\leq C \|\Sigma_1 - \Sigma_2\|_{\text{op}} + C \|\hat{\Sigma}_1 - \hat{\Sigma}_2\|_{\text{op}}
\end{aligned}$$

Let $\hat{\Sigma}_1 = n^{-1}X_1'X_1$ and $\hat{\Sigma}_2 = n^{-1}X_2'X_2$. Then,

$$\begin{aligned}
|F_n(z; \hat{\Sigma}_1, \Sigma_1) - F_n(z; \hat{\Sigma}_2, \Sigma_2)| &\leq C \|\Sigma_1 - \Sigma_2\|_{\text{op}} + \frac{C}{n} \|X_1'X_1 - X_1'X_2 + X_1'X_2 - X_2'X_2\|_{\text{op}} \\
&\leq C \|\Sigma_1 - \Sigma_2\|_{\text{op}} + \frac{C}{n} \|X_1'(X_1 - X_2) + (X_1 - X_2)'X_2\|_{\text{op}} \quad (27) \\
&\leq C \|\Sigma_1 - \Sigma_2\|_{\text{op}} + \frac{C}{n} \|X_1 - X_2\|_{\text{op}} (\|X_1\|_{\text{op}} + \|X_2\|_{\text{op}})
\end{aligned}$$

The rest of the proof relies on the same truncation and centralization arguments used in [Hastie et al. \(2020\)](#) (Appendix A.4.).

Let $M > 0$. We decompose the matrices of covariates, X , and latent covariates, Z , as follows:

$$\begin{aligned}
X &= X_M + \tilde{X}_M, \quad X_M = Z_M \Sigma_M^{1/2}, \quad \tilde{X}_M = \tilde{Z}_M \Sigma^{1/2} \\
Z &= a_M Z_M + \tilde{Z}_M \\
\Sigma_M &= a_M^2 \Sigma
\end{aligned}$$

where, denoting by Z_{ij} the (i, j) -th entry of Z ,

$$\begin{aligned}
(Z_M)_{ij} &= \frac{1}{a_M} \left(Z_{ij} \mathbf{1}_{|Z_{ij}| \leq M} - \mathbb{E}[Z_{ij} \mathbf{1}_{|Z_{ij}| \leq M}] \right), \quad a_M = \mathbb{E} \left[\left(Z_{ij} \mathbf{1}_{|Z_{ij}| \leq M} - \mathbb{E}[Z_{ij} \mathbf{1}_{|Z_{ij}| \leq M}] \right)^2 \right]^{1/2} \\
(\tilde{Z}_M)_{ij} &= Z_{ij} \mathbf{1}_{|Z_{ij}| > M} - \mathbb{E}[Z_{ij} \mathbf{1}_{|Z_{ij}| > M}]
\end{aligned}$$

Note that $Z_{ij} = a_M (Z_M)_{ij} + (\tilde{Z}_M)_{ij}$. Each entry of Z_M and \tilde{Z}_M has zero mean and the entries of Z_M have unit variance and are bounded. Moreover, the fourth moment of Z_{ij} are finite, which entails

$$|a_M^2 - 1| \leq \varepsilon_M, \quad \mathbb{E} \left[\left| (\tilde{Z}_M)_{ij} \right|^4 \right] \leq \varepsilon_M^4$$

for some $\varepsilon_M \rightarrow 0$ as $M \rightarrow \infty$.

Using (27), we obtain

$$\begin{aligned} |F_n(z; \hat{\Sigma}_1, \Sigma_1) - F_n(z; \hat{\Sigma}_2, \Sigma_2)| &\leq C \|\Sigma_M - \Sigma\|_{\text{op}} + \frac{C}{n} \|\tilde{X}_M\|_{\text{op}} \left(\|X\|_{\text{op}} + \|X_M\|_{\text{op}} \right) \\ &\leq C\tau^{-1} |a_M^2 - 1| + C\tau^{-1} \left\| \frac{\tilde{Z}_M}{\sqrt{n}} \right\|_{\text{op}} \left(\left\| \frac{Z}{\sqrt{n}} \right\|_{\text{op}} + \left\| \frac{Z_M}{\sqrt{n}} \right\|_{\text{op}} \right) \end{aligned}$$

Recall that the operator norm of a real matrix Y is the square root of the maximum eigenvalue of the (symmetric) matrix $Y'Y$. Therefore, Lemma 3 ensures that

$$\limsup_{n,p \rightarrow \infty} \left(\left\| \frac{Z}{\sqrt{n}} \right\|_{\text{op}} + \left\| \frac{Z_M}{\sqrt{n}} \right\|_{\text{op}} \right) \leq K < \infty, \quad \limsup_{n,p \rightarrow \infty} \left\| \frac{\tilde{Z}_M}{\sqrt{n}} \right\|_{\text{op}} < K\varepsilon_M, \quad a.s.$$

which yields

$$\limsup_{n,p \rightarrow \infty} |F_n(z; \hat{\Sigma}, \Sigma) - F_n(z; n^{-1} X'_M X_M, \Sigma_M)| \leq C\tau^{-1} K\varepsilon_M = C_1\varepsilon_M \quad (28)$$

Next, denote by μ^M and ζ_d^M the ESD and reweighted ESD of Σ_M defined analogously to the measures in (22) and (24) for Σ .

As each entry of Z_M has bounded moments of all orders, we can apply Lemma 2 to $F_n(z; n^{-1} X'_M X_M, \Sigma_M)$. Then, taking $\varepsilon = 0.1$ and $D = 2$, we have

$$|F_n(z; n^{-1} X'_M X_M, \Sigma_M) - \bar{F}_n(z; \mu^M, \zeta_d^M)| \leq \frac{\|\Sigma_M \beta_{\text{OOS}}\| \|\beta_{\text{IS}}\|}{n^{0.49} z} = \frac{C}{n^{0.49}}$$

with probability $1 - n^{-2}$ for n large enough.

Concomitantly, we have the following relations for the spectral measures:

$$\mu^M(x) = \mu\left(\frac{x}{a_M^2}\right), \quad \zeta_d^M(x) = \zeta_d\left(\frac{x}{a_M^2}\right)$$

Therefore, $\mu^M(x)$ (resp. $\zeta_d^M(x)$) converges weakly to $\nu^M(x) = \nu(x/a_M^2)$ (resp. $\eta_d^M(x) = \eta_d(x/a_M^2)$). By Borel-Cantelli lemma, this yields

$$\limsup_{n \rightarrow \infty} |F_n(z; n^{-1} X'_M X_M, \Sigma_M) - \bar{F}_n(z; \nu^M, \eta_d^M)| = 0. \quad (29)$$

Finally, note that ν^M (resp. η_d^M) weakly converges to ν (resp. η_d) as $M \rightarrow \infty$. Consequently, taking $M \rightarrow \infty$, Equations (28) and (29) yield

$$F_n(z; \hat{\Sigma}, \Sigma) \xrightarrow{a.s.} \bar{F}_n(z; \nu, \eta_d)$$

The proof of Lemma 4 is complete. \square

Lemma 5. Let $\xi = (e_1, e_2, \dots, e_n)'$ with $(e_i)_i$ as in (1). Then,

$$\frac{1}{n^2} \mathbb{E}[(X'\xi)(X'\xi)'|X] = \frac{1}{n} \hat{\Sigma}$$

Proof.

$$\begin{aligned} \frac{1}{n^2} \mathbb{E}[(X'\xi)(X'\xi)'|X] &= \frac{1}{n^2} X' \mathbb{E}[\xi \xi' | X] X = \frac{1}{n^2} X' \mathbb{E}[\xi \xi'] X \\ &= \frac{1}{n^2} X' X = \frac{1}{n} \hat{\Sigma} \end{aligned}$$

\square

Lemma 6. Let $z > 0$, $\xi = (e_1, e_2, \dots, e_n)'$ with $(e_i)_i$ as in (1) and Assumptions (2.1), (2.2), (A.1) hold. Besides, assume $\mathbb{E}[\lambda_{\max}(n^{-1}Z'Z)] \leq K < \infty$, for any $n \in \mathbb{N}_{>0}$. Then, there exist $C := C(\tau, K)$ such that with probability at least $1 - n^{-1/5}$,

$$\left| \frac{1}{n} \beta'_{\text{oos}} \Sigma (zI + \hat{\Sigma})^{-1} X' \xi \right| \leq \frac{C \|\Sigma \beta_{\text{oos}}\|}{n^{2/5}}$$

Proof. Using Chebyshev's inequality, for some $t > 0$, we have

$$\mathbb{P}\left(\left|\frac{1}{n} \beta'_{\text{oos}} \Sigma (zI + \hat{\Sigma})^{-1} X' \xi\right|^2 \geq t\right) \leq \frac{\mathbb{V}\left[\frac{1}{n} \beta'_{\text{oos}} \Sigma (zI + \hat{\Sigma})^{-1} X' \xi\right]}{t^2} = \frac{\mathbb{E}\left[\left|\frac{1}{n} \beta'_{\text{oos}} \Sigma (zI + \hat{\Sigma})^{-1} X' \xi\right|^2\right]}{t^2} \quad (30)$$

The equality follows from the independence of X and ξ . Besides,

$$\begin{aligned} \mathbb{E}\left[\left|\frac{1}{n} \beta'_{\text{oos}} \Sigma (zI + \hat{\Sigma})^{-1} X' \xi\right|^2\right] &= \mathbb{E}\left[\left(\frac{1}{n} \beta'_{\text{oos}} \Sigma (zI + \hat{\Sigma})^{-1} X' \xi\right) \left(\frac{1}{n} \beta'_{\text{oos}} \Sigma (zI + \hat{\Sigma})^{-1} X' \xi\right)'\right] \\ &= \frac{1}{n^2} \mathbb{E}\left[\beta'_{\text{oos}} \Sigma (zI + \hat{\Sigma})^{-1} X' \xi \xi' X (zI + \hat{\Sigma})^{-1} \Sigma \beta_{\text{oos}}\right] \\ &= \mathbb{E}\left[\beta'_{\text{oos}} \Sigma (zI + \hat{\Sigma})^{-1} \frac{1}{n^2} \mathbb{E}[(X'\xi)(X'\xi)'|X] (zI + \hat{\Sigma})^{-1} \Sigma \beta_{\text{oos}}\right] \end{aligned}$$

The last equality results from the law of iterated expectations. Next, using Lemma 5, we have

$$\begin{aligned}
\mathbb{E} \left[\left| \frac{1}{n} \beta'_{oos} \Sigma (zI + \hat{\Sigma})^{-1} X' \xi \right|^2 \right] &= \frac{1}{n} \mathbb{E} \left[\beta'_{oos} \Sigma (zI + \hat{\Sigma})^{-1} \hat{\Sigma} (zI + \hat{\Sigma})^{-1} \Sigma \beta_{oos} \right] \\
&= \frac{1}{n} \beta'_{oos} \Sigma \mathbb{E} \left[(zI + \hat{\Sigma})^{-1} \Sigma^{1/2} \left(\frac{1}{n} Z' Z \right) \Sigma^{1/2} (zI + \hat{\Sigma})^{-1} \right] \Sigma \beta_{oos} \\
&\leq \frac{1}{n} \|\Sigma \beta_{oos}\|^2 \|\Sigma^{1/2}\|_{\text{op}}^2 \mathbb{E} \left[\|(zI + \hat{\Sigma})^{-1}\|_{\text{op}}^2 \left\| \frac{1}{n} Z' Z \right\|_{\text{op}} \right] \\
&\leq \frac{1}{n} \|\Sigma \beta_{oos}\|^2 \tau^{-1} z^{-2} \mathbb{E} \left[\left\| \frac{1}{n} Z' Z \right\|_{\text{op}} \right] \\
&= \frac{C \|\Sigma \beta_{oos}\|^2}{nz^2}
\end{aligned} \tag{31}$$

Taking $t = C^{1/2} \|\Sigma \beta_{oos}\| n^{-2/5} z$ in (30), we get

$$\mathbb{P} \left(\left| \frac{1}{n} \beta'_{oos} \Sigma (zI + \hat{\Sigma})^{-1} X' \xi \right| \geq \frac{C^{1/2} \|\Sigma \beta_{oos}\|}{n^{2/5} z} \right) \leq \frac{1}{n^{1/5}}$$

□

Corollary 1. Let $z > 0$, $\xi = (e_1, e_2, \dots, e_n)'$ with $(e_i)_i$ as in (1) and Assumptions (2.1), (2.2), (A.1) hold. Then, in the limit, as $p, n \rightarrow \infty$, $p/n \rightarrow c \in (0, \infty)$,

$$\frac{1}{n} \beta'_{oos} \Sigma (zI + \hat{\Sigma})^{-1} X' \xi \xrightarrow{L_2} 0$$

Proof. Using Bai-Yin theorem (Yin et al. (1988), Bai and Yin (2008)), we have $\limsup_{n,p \rightarrow \infty} \|n^{-1} Z' Z\|_{\text{op}} \leq K < \infty$. Then, the result follows from taking $n \rightarrow \infty$ in (31). □

Proposition 4. Let $z > \tau$, $\xi = (e_1, e_2, \dots, e_n)'$ with $(e_i)_i$ as in (1) and Assumptions (2.1), (2.2), (A.1), (A.2) hold. Then, there exists $C := C(\tau)$ such that

$$\left| \mathbb{E} \left[r_{t+1}^{(s)}(z) | X \right] - (\bar{H}_n(\zeta_d) + \bar{F}_n(z; \mu, \zeta_d)) \right| \leq \frac{C \|\beta_{is}\| \|\beta_{oos}\|}{n^{2/5} z} \tag{32}$$

holds with probability at least $1 - n^{-1/5}$ for n sufficiently large.

Proof. We wish to study the out-of-sample expected return of the market timing strategy. Then, we integrate over the randomness in a new (independent) observation $x_t \in \mathbb{R}^p$ and in the errors $e_t \in \mathbb{R}$. Therefore,

$$\begin{aligned}
\mathbb{E} \left[r_{t+1}^{(s)}(z) | X \right] &= \mathbb{E} [\hat{\pi}_t r_{t+1} | X] \\
&= \mathbb{E} [\hat{\beta}'_{is} x_t (x'_t \beta_{oos} + e_t) | X] \\
&= \mathbb{E} [\hat{\beta}'_{is} x_t x'_t \beta_{oos} | X] \\
&= \mathbb{E} [\beta'_{oos} x_t x'_t \hat{\beta}_{is} | X]
\end{aligned} \tag{33}$$

Let $\xi = (e_{t-n-1}, e_{t-n}, \dots, e_{t-1})'$. Then,

$$\begin{aligned}\hat{\beta}_{is} &= \frac{1}{n}(zI + \hat{\Sigma})^{-1}X'(X\beta_{is} + \xi) \\ &= (zI + \hat{\Sigma})^{-1}(\hat{\Sigma}\beta_{is} + \frac{1}{n}X'\xi)\end{aligned}\tag{34}$$

Injecting this into (33), we get

$$\begin{aligned}\mathbb{E}\left[r_{t+1}^{(s)}(z)|X\right] &= \mathbb{E}[\beta'_{oos}x_t x'_t(zI + \hat{\Sigma})^{-1}(\hat{\Sigma}\beta_{is} + \frac{1}{n}X'\xi)|X] \\ &= \mathbb{E}[\beta'_{oos}x_t x'_t(zI + \hat{\Sigma})^{-1}\hat{\Sigma}\beta_{is}|X] + \mathbb{E}\left[\frac{1}{n}\beta'_{oos}x_t x'_t(zI + \hat{\Sigma})^{-1}X'\xi|X\right] \\ &= \beta'_{oos}\mathbb{E}[x_t x'_t](zI + \hat{\Sigma})^{-1}\hat{\Sigma}\beta_{is} + \frac{1}{n}\beta'_{oos}\mathbb{E}[x_t x'_t](zI + \hat{\Sigma})^{-1}X'\xi \\ &= \beta'_{oos}\Sigma(zI + \hat{\Sigma})^{-1}\hat{\Sigma}\beta_{is} + \frac{1}{n}\beta'_{oos}\Sigma(zI + \hat{\Sigma})^{-1}X'\xi \\ &= \beta'_{oos}\Sigma(zI + \hat{\Sigma})^{-1}(\hat{\Sigma} + zI - zI)\beta_{is} + \frac{1}{n}\beta'_{oos}\Sigma(zI + \hat{\Sigma})^{-1}X'\xi \\ &= \beta'_{oos}\Sigma\beta_{is} - z\beta'_{oos}\Sigma(zI + \hat{\Sigma})^{-1}\beta_{is} + \frac{1}{n}\beta'_{oos}\Sigma(zI + \hat{\Sigma})^{-1}X'\xi.\end{aligned}$$

The inequality (32) follows from Lemma 6 and by taking $\varepsilon = 10^{-1}$ and $D = 1/5$ in Lemma 2. \square

We define the limiting out-of-sample expected return of the strategy under concept drift if the model is well-specified

$$\begin{aligned}\mathcal{E}^{(d)}(z; c, \nu, \eta_d) &= \langle \beta_{oos}, \beta_{is} \rangle_{Q(z)} \\ &= \|\beta_{is}\| \|\beta_{oos}\| \int \left(\lambda - \frac{z\lambda}{\lambda(czm_n(-z; c, \mu) + 1 - c) + z} \right) d\eta_d(\lambda)\end{aligned}\tag{35}$$

with $Q(z) \equiv Q(z; c, \Sigma) := \Sigma(I - z(zI + (czm_n(-z; c, \mu) + 1 - c)\Sigma)^{-1})$ and $m_n := m_n(-z; c, \mu)$ is given in Definition 4.

Proposition 5. *Let $z > \tau$ and Assumptions (2.1), (2.2), (A.1), (A.2), (A.3), (A.4) hold. Then,*

$$\mathbb{E}\left[r_{t+1}^{(s)}(z)|X\right] \xrightarrow[\substack{n, p \rightarrow \infty \\ p/n \rightarrow c}]{\mathbb{P}} \mathcal{E}^{(d)}(z; c, \nu, \eta_d)$$

Proof. By Lemma 4, we have

$$-z\beta'_{oos}\Sigma(zI + \hat{\Sigma})^{-1}\beta_{is} \xrightarrow[\substack{\text{a.s.} \\ n, p \rightarrow \infty \\ p/n \rightarrow c}]{-z\beta'_{oos}\Sigma(zI + (czm_n(-z; c, \mu) + 1 - c)\Sigma)^{-1}\beta_{is},$$

and by Corollary 1,

$$\frac{1}{n} \beta'_{oos} \Sigma (zI + \hat{\Sigma})^{-1} X' \xi \xrightarrow[n, p \rightarrow \infty]{p/n \rightarrow c} 0.$$

Consequently,

$$\mathbb{E} \left[r_{t+1}^{(s)}(z) | X \right] \xrightarrow[n, p \rightarrow \infty]{p/n \rightarrow c} \beta'_{oos} \Sigma \beta_{is} - z \beta'_{oos} \Sigma (zI + (czm_n(-z; c, \mu) + 1 - c) \Sigma)^{-1} \beta_{is}$$

The proof of Proposition 5 is complete. \square

We define the limiting out-of-sample expected return of the strategy when the model is well-specified and no concept drift is considered:

$$\begin{aligned} \mathcal{E}(z; c, \nu, \eta_{is}) &= \|\beta_{is}\|_{Q(z)}^2 \\ &= \|\beta_{is}\|^2 \int \left(\lambda - \frac{z\lambda}{\lambda(czm_n(-z; c, \mu) + 1 - c) + z} \right) d\eta_{is}(\lambda) \end{aligned} \quad (36)$$

with $Q(z) \equiv Q(z; c, \Sigma) := \Sigma(I - z(zI + (czm_n(-z; c, \mu) + 1 - c)\Sigma)^{-1})$ and $m_n := m_n(-z; c, \mu)$ is given in Definition 4.

Corollary 2. *Let $z > \tau$ and Assumptions (2.1), (2.2), (A.1), (A.2), (A.3), (A.4) hold. Then,*

$$\mathbb{E} \left[r_{t+1}^{(s)}(z) | X, \beta_{is} = \beta_{oos} \right] \xrightarrow[n, p \rightarrow \infty]{p/n \rightarrow c} \mathcal{E}(z; c, \nu, \eta_{is}).$$

Proof. The proof is straightforward from Proposition 5. \square

Lemma 7. *Let $z > \tau$ and Assumptions (2.1), (2.2), (A.1), (A.2), (A.3), (A.4) hold.*

$$\mathcal{E}^{(d)}(z; c, \nu, \eta_d) = \frac{1}{2} \left(\|\beta_{oos}\|_{Q(z)}^2 + \|\beta_{is}\|_{Q(z)}^2 - \|\beta_{is} - \beta_{oos}\|_{Q(z)}^2 \right)$$

where $Q(z) \equiv Q(z; c, \Sigma) := \Sigma(I - z(zI + (czm_n(-z; c, \mu) + 1 - c)\Sigma)^{-1})$, or alternatively

$$\begin{aligned} \mathcal{E}^{(d)}(z; c, \nu, \eta_d) &= \frac{\|\beta_{is}\|^2}{2} \int \left(\lambda - \frac{z\lambda}{\lambda(czm_n(-z; c, \mu) + 1 - c) + z} \right) d\eta_{is}(\lambda) \\ &\quad + \frac{\|\beta_{oos}\|^2}{2} \int \left(\lambda - \frac{z\lambda}{\lambda(czm_n(-z; c, \mu) + 1 - c) + z} \right) d\eta_{oos}(\lambda) \\ &\quad - \frac{\|\beta_{is} - \beta_{oos}\|^2}{2} \int \left(\lambda - \frac{z\lambda}{\lambda(czm_n(-z; c, \mu) + 1 - c) + z} \right) d\eta_r(\lambda). \end{aligned}$$

Proof. This result follows from the polarization identity $\langle (u-v), A(u-v) \rangle = \langle u, Au \rangle + \langle v, Av \rangle - 2\langle u, Av \rangle$ for $u, v \in \mathbb{R}^p$ and $0 \preceq A \in \mathbb{R}^{p \times p}$. \square

The following proposition establishes the conditions under which the performance of the strategy deteriorates in the presence of concept drift.

Proposition 6. Let $z > \tau$ and Assumptions (2.1), (2.2), (A.1), (A.2), (A.3), (A.4) hold. Consider $\mathcal{E}^{(d)}(z; c, \nu, \eta_d)$ and $\mathcal{E}(z; c, \nu, \eta_{is})$ as defined in (35) and (36) respectively. Then,

$$\mathcal{E}^{(d)}(z; c, \nu, \eta_d) < \mathcal{E}(z; c, \nu, \eta_{is})$$

if and only if,

$$\langle (\beta_{oos} - \beta_{is}), \beta_{is} \rangle_{Q(z)} < 0 \quad (37)$$

or alternatively, if and only if,

$$\|\beta_{oos}\|_{Q(z)}^2 - \|\beta_{is}\|_{Q(z)}^2 < \|\beta_{is} - \beta_{oos}\|_{Q(z)}^2 \quad (38)$$

Proof. Condition (37) directly follows from the definition of $\mathcal{E}^{(d)}(z; c, \nu, \eta_d)$ and $\mathcal{E}(z; c, \nu, \eta_{is})$, i.e.,

$$\begin{aligned} \mathcal{E}^{(d)}(z; c, \nu, \eta_d) &< \mathcal{E}(z; c, \nu, \eta_{is}) \\ \Leftrightarrow \langle \beta_{oos}, \beta_{is} \rangle_{Q(z)} &< \|\beta_{is}\|_{Q(z)}^2 \\ \Leftrightarrow \langle \beta_{oos}, Q(z)\beta_{is} \rangle &< \langle \beta_{is}, Q(z)\beta_{is} \rangle \\ \Leftrightarrow \langle (\beta_{oos} - \beta_{is}), Q(z)\beta_{is} \rangle &< 0 \\ \Leftrightarrow \langle (\beta_{oos} - \beta_{is}), \beta_{is} \rangle_{Q(z)} &< 0 \end{aligned}$$

Next, we use Lemma 7 to derive Condition (38). Indeed, note that we can rewrite $\mathcal{E}^{(d)}(z; c, \nu, \eta_d)$ as

$$\mathcal{E}^{(d)}(z; c, \nu, \eta_d) = \mathcal{E}(z; c, \nu, \eta_{is}) + \frac{1}{2} \left(\|\beta_{oos}\|_{Q(z)}^2 - \|\beta_{is}\|_{Q(z)}^2 - \|\beta_{is} - \beta_{oos}\|_{Q(z)}^2 \right).$$

Then,

$$\begin{aligned} \mathcal{E}^{(d)}(z; c, \nu, \eta_d) &< \mathcal{E}(z; c, \nu, \eta_{is}) \\ \Leftrightarrow \frac{1}{2} \left(\|\beta_{oos}\|_{Q(z)}^2 - \|\beta_{is}\|_{Q(z)}^2 - \|\beta_{is} - \beta_{oos}\|_{Q(z)}^2 \right) &< 0 \\ \Leftrightarrow \|\beta_{oos}\|_{Q(z)}^2 - \|\beta_{is}\|_{Q(z)}^2 &< \|\beta_{is} - \beta_{oos}\|_{Q(z)}^2 \end{aligned}$$

The proof of Proposition 6 is complete. \square

The next proposition establishes the limiting out-of-sample expected return of the strategy under concept drift in the standard isotropic scenario, i.e. the covariates are i.i.d. with $\Sigma = I$.

Proposition 7. Let $z > \tau$. Assume $x_i = (x_{i1}, x_{i2}, \dots, x_{ip})$ has independent and identically distributed entries and, in addition, that for all $j \in \{1, \dots, p\}$, $\mathbb{E}[z_{ij}] = 0$, $\mathbb{E}[z_{ij}^2] = 1$ and $\mathbb{E}[|z_{ij}|^{4+a}] \leq C < \infty$ for $a > 0$. Then,

$$\mathbb{E} \left[r_{t+1}^{(s)}(z) \middle| X \right] \xrightarrow[n, p \rightarrow \infty]{p/n \rightarrow c} f(z; c) \langle \beta_{is}, \beta_{oos} \rangle$$

where

$$f(z; c) = 1 - \frac{z}{z(1 + cm(-z; c)) + 1 - c} \in [0, 1),$$

$$\text{with } m(-z; c) = \frac{c - 1 - z + \sqrt{(1 - c + z)^2 + 4cz}}{2cz}. \quad (39)$$

Furthermore, $z \mapsto f(z; c)\langle \beta_{is}, \beta_{oos} \rangle$ is monotone decreasing (resp. increasing) in z when $\langle \beta_{is}, \beta_{oos} \rangle \geq 0$ (resp. $\langle \beta_{is}, \beta_{oos} \rangle \leq 0$).

Proof. Let $\Sigma = I$. Then,

$$\mathcal{E}^{(d)}(z; c, \nu, \eta_d) = \beta'_{oos} Q(I) \beta_{is}$$

with

$$\begin{aligned} Q(I) &= I(I - z(zI + (czm_n(-z; c, \mu) + 1 - c)I)^{-1}) \\ &= \left(1 - \frac{z}{z + czm_n(-z; c, \mu) + 1 - c}\right) I \end{aligned}$$

We are left with finding $m_n(-z; c, \mu)$ with $\Im(-z) > 0$. Recall that $m_n := m_n(-z; c, \mu)$ is the unique solution in \mathbb{C}_+ to

$$\begin{aligned} m_n &= \int \frac{1}{\lambda(1 - c + czm_n) + z} d\mu(\lambda) \\ &= \frac{1}{p} \sum_{i=1}^p \frac{1}{1 - c + czm_n + z} \\ &= \frac{1}{1 - c + czm_n + z} \end{aligned}$$

This is a quadratic equation in m_n whose roots are:

$$m_n = \frac{c - 1 - z \pm \sqrt{(1 - c + z)^2 + 4cz}}{2cz}.$$

By the definition of the Stieltjes transform, $m_n(-z)$ must behave like $1/z$ as $|z| \rightarrow \infty$. This is only possible when the positive branch cut is chosen. This yields:

$$m(-z; c) = \frac{c - 1 - z + \sqrt{(1 - c + z)^2 + 4cz}}{2cz}.$$

Note that the quantity $czm_n(-z; c) + 1 - c$ is always positive. Indeed,

$$\begin{aligned}
& czm_n(-z; c) + 1 - c > 0 \\
\Leftrightarrow & c - 1 - z + \sqrt{(1 - c + z)^2 + 4cz} > 2(c - 1) \\
\Leftrightarrow & (1 - c + z)^2 - (1 - c - z)^2 + 4cz > 0 \\
\Leftrightarrow & 4z(1 - c) + 4cz > 0 \\
\Leftrightarrow & z > 0
\end{aligned}$$

which is always verified as $z > \tau > 0$. Therefore,

$$f(z; c) = 1 - \frac{z}{z(1 + cm(-z; c)) + 1 - c} \in [0, 1).$$

Regarding the monotonicity of the limiting expected return in z , notice that

$$\begin{aligned}
m(z; c) &= \frac{1}{1 - c - czm(z; c) - z} \\
\Rightarrow m'(z; c) &= \frac{cm(z; c) + czm'(z; c) + 1}{(1 - c - czm(z; c) - z)^2} \\
\Rightarrow m'(z; c) &= \frac{1 + cm(z; c)}{[1 - c - czm(z; c) - z]^2 - cz}.
\end{aligned}$$

Hence,

$$m'(-z; c) = \frac{1 + cm(-z; c)}{[1 - c + czm(-z; c) + z]^2 + cz} \geq 0.$$

Finally, we have

$$\frac{\partial}{\partial z} \left[\left(1 - \frac{z}{z(1 + cm(-z; c)) + 1 - c} \right) \langle \beta_{is}, \beta_{oos} \rangle \right] = - \frac{cm'(-z; c)z^2 + 1 + c}{[z(1 + cm(-z; c)) + 1 - c]^2} \langle \beta_{is}, \beta_{oos} \rangle. \quad (40)$$

The derivative in (40) is negative (resp. positive) when $\langle \beta_{is}, \beta_{oos} \rangle \geq 0$ (resp. $\langle \beta_{is}, \beta_{oos} \rangle \leq 0$), and the proof of Proposition 7 is complete. \square

A.5.2 Well-specified model and ridgeless regression

In this subsection, we extend the results presented in the previous subsection to the ridgeless case, i.e. taking $z \rightarrow 0$. Here again, we consider that the true model is known. Hence, $\theta = 0$, $q = 0$, $\phi = 1$ and $\Sigma \equiv \Sigma_x$.

Let

$$G_n = \lim_{z \rightarrow 0} -z \langle \beta_{oos}, \Sigma(\hat{\Sigma} + zI)^{-1} \beta_{is} \rangle,$$

and define:

$$\begin{aligned}\bar{G}_n(\mu, \zeta_d) &= -\langle \beta_{oos}, \Sigma(I + cs_0\Sigma)^{-1}\beta_{is} \rangle \\ &= -\|\beta_{is}\| \|\beta_{oos}\| \int \frac{\lambda}{1 + \lambda cs_0} d\zeta_d(\lambda),\end{aligned}$$

where $s_0 := s_0(c, \mu)$ is given in Definition 5.

Moreover, consider the following hypothesis.

Assumption A.6. $|c - 1| \geq \tau$.

The complexity of the model is supposed to be bounded away from the interpolation threshold, $c = 1$.

Assumption A.7. $\lambda_p > \tau$.

This assumption imposes positive-definiteness to Σ by requiring the minimum eigenvalue of the covariance matrix to be strictly positive.

We now state a number of lemmas that will be useful in the remainder of the proofs. In particular, Lemma 9 establishes non-asymptotic bounds for the gap between G_n and \bar{G}_n .

Lemma 8. *Let Assumptions (2.2), (A.1), (A.2), (A.5), (A.6) and (A.7) hold. Define $s_n(-z; c, \mu) = m_n(-z; c, \mu) - (c-1)/cz$ where $m_n(-z; c, \mu)$ is given in Definition 4 and $s_0(c, \mu) = \lim_{z \rightarrow 0} s_n(-z; c, \mu)$ which is given in Definition 5. Then,*

$$m_n(-z; c, \mu) = \frac{c-1}{cz} + s_0(c, \mu) + O_*(z),$$

where $O_*(z)$ denotes a quantity uniformly bounded as $|O_*(z)| \leq C(\tau)z$.

Proof. The proof is given in Appendix B.1. in [Hastie et al. \(2020\)](#). □

Lemma 9. *Let Assumptions (2.2), (A.1), (A.2), (A.5), (A.6) and (A.7) hold. Then, for any $D > 0$ and $\varepsilon > 0$, there exist $C := C(\tau)$ and $n_0 := n_0(\varepsilon, D)$ such that for $n \geq n_0$,*

$$|G_n - \bar{G}_n(\mu, \zeta_d)| \leq \frac{C \|\beta_{oos}\| \|\beta_{is}\|}{n^{\frac{1}{4}-\varepsilon}}, \quad (41)$$

holds with probability $1 - n^{-D}$.

Proof. We proceed in three steps. First, we show that $|G_n - F_n(z)| \leq C(\tau) \|\beta_{oos}\| \|\beta_{is}\| z$. Then, we show that $|\bar{G}_n(\mu, \zeta_d) - \bar{F}_n(z; \mu, \zeta_d)| \leq C(\tau) \|\beta_{oos}\| \|\beta_{is}\| z$. Finally, using Lemma 2 and combining both results, we prove the desired bound.

1) Bound on $|G_n - F_n(z)|$.

$$\begin{aligned}
|G_n - F_n(z)| &= \left| \lim_{z \rightarrow 0} \left(-z\beta'_{oos}\Sigma(\hat{\Sigma} + zI)^{-1}\beta_{is} \right) + z\beta'_{oos}\Sigma(zI + \hat{\Sigma})^{-1}\beta_{is} \right| \\
&= \left| \lim_{z \rightarrow 0} \left(-z\beta'_{oos}\Sigma(\hat{\Sigma} + zI)^{-1}\beta_{is} \right) + \beta'_{oos}\Sigma\beta_{is} \right. \\
&\quad \left. - \beta'_{oos}\Sigma\beta_{is} + z\beta'_{oos}\Sigma(zI + \hat{\Sigma})^{-1}\beta_{is} \right| \\
&= \left| \lim_{z \rightarrow 0} \left(\beta'_{oos}\Sigma(\hat{\Sigma} + zI)^{-1}\hat{\Sigma}\beta_{is} \right) - \beta'_{oos}\Sigma(zI + \hat{\Sigma})^{-1}\hat{\Sigma}\beta_{is} \right| \\
&= \left| \beta'_{oos}\Sigma\hat{\Sigma}^+\hat{\Sigma}\beta_{is} - \beta'_{oos}\Sigma(zI + \hat{\Sigma})^{-1}\hat{\Sigma}\beta_{is} \right|.
\end{aligned} \tag{42}$$

Denote by $r_1 \geq r_2 \geq \dots \geq r_p \geq 0$ the eigenvalues of $\hat{\Sigma}$. Let $\hat{\Sigma} = PDP^{-1}$ be the eigen-decomposition of $\hat{\Sigma}$. Then, $P \in \mathbb{R}^{p \times p}$ is orthogonal and $D \in \mathbb{R}^{p \times p}$ is a diagonal matrix with the eigenvalues of $\hat{\Sigma}$ on the main diagonal. By construction, $\hat{\Sigma}^+ = PEP^{-1}$ with E a diagonal matrix such that

$$E_{ii} = \begin{cases} r_i^{-1}, & r_i > 0 \\ 0, & r_i = 0. \end{cases}$$

Therefore, we have $\hat{\Sigma}^+\hat{\Sigma} = PEDP^{-1} = PQP^{-1}$ with Q diagonal such that, for any $i \in \{1, \dots, p\}$, $Q_{ii} = 1$ if $r_i > 0$ and 0 otherwise. Coming back to (42), we have

$$\begin{aligned}
|G_n - F_n(z)| &= \left| \beta'_{oos}\Sigma\hat{\Sigma}^+\hat{\Sigma}\beta_{is} - \beta'_{oos}\Sigma(zI + \hat{\Sigma})^{-1}\hat{\Sigma}\beta_{is} \right| \\
&= \left| \beta'_{oos}\Sigma P \left(Q - (zI + D)^{-1}D \right) P^{-1}\beta_{is} \right|.
\end{aligned}$$

Let $T = Q - (zI + D)^{-1}D$. Then, $T \in \mathbb{R}^{p \times p}$ is a diagonal matrix such that

$$T_{ii} = \begin{cases} \frac{z}{r_i + z}, & r_i > 0 \\ 0, & r_i = 0. \end{cases}$$

Hence, introducing r_{\min} and $\lambda_{\min}(n^{-1}Z'Z)$ the smallest non-vanishing eigenvalues of $\hat{\Sigma}$ and $n^{-1}Z'Z$ respectively, we get the following bound

$$\begin{aligned}
|G_n - F_n(z)| &= \left| \beta'_{oos}\Sigma P T P^{-1}\beta_{is} \right| \\
&\leq \|\beta_{oos}\| \|\Sigma\|_{\text{op}} \|P\|_{\text{op}}^2 \|T\|_{\text{op}} \|\beta_{is}\| \\
&\leq \|\beta_{oos}\| \|\beta_{is}\| \tau^{-1} \frac{z}{r_{\min}} \\
&\leq \|\beta_{oos}\| \|\beta_{is}\| \tau^{-1} \frac{z}{\|\Sigma^{1/2}\|_{\text{op}}^2 \lambda_{\min}(n^{-1}Z'Z)} \\
&\leq \|\beta_{oos}\| \|\beta_{is}\| \tau^{-2} \frac{z}{\lambda_{\min}(n^{-1}Z'Z)}.
\end{aligned}$$

By Assumption (A.6), the Bai-Yin theorem (Bai and Yin (2008)) yields that $\lambda_{\min}(n^{-1}Z'Z) \geq \kappa(\tau) > 0$ with probability at least $1 - n^{-D}$ for any $D > 0$ and n sufficiently large. Finally, with the same probability, we have

$$\begin{aligned} |G_n - F_n(z)| &\leq \|\beta_{oos}\| \|\beta_{is}\| \tau^{-2} \frac{z}{\kappa(\tau)} \\ &\leq C(\tau) \|\beta_{oos}\| \|\beta_{is}\| z. \end{aligned}$$

2) Bound on $|\bar{G}_n(\mu, \zeta_d) - \bar{F}_n(z; \mu, \zeta_d)|$.

Recall the following fundamental relation presented in Equation (26)

$$r_n(-z) = cm_n(-z; c, \mu) + \frac{1-c}{z},$$

or equivalently,

$$m_n(-z; c, \mu) = s_n(-z; c, \mu) + \frac{c-1}{cz}. \quad (43)$$

with $s_n(-z; c, \mu) = r_n(-z)/c$. Let $s_0(c, \mu) = \lim_{z \rightarrow 0} s_n(-z; c, \mu)$. According to Lemma 8, we have

$$m_n(-z; c, \mu) = \frac{c-1}{cz} + s_0(c, \mu) + O_*(z)$$

where $O_*(z)$ denotes a quantity uniformly bounded as $|O_*(z)| \leq C(\tau)z$.

Injecting this into $\bar{F}_n(z; \mu, \zeta_d)$, we get

$$\begin{aligned} \frac{\bar{F}_n(z; \mu, \zeta_d)}{\|\beta_{is}\| \|\beta_{oos}\|} &= -z \int \frac{\lambda}{\lambda(czm_n(-z; c, \mu) + 1 - c) + z} d\zeta_d(\lambda) \\ &= -z \int \frac{\lambda}{\lambda(cz[(c-1)/cz + s_0(c, \mu) + O_*(z)] + 1 - c) + z} d\zeta_d(\lambda) \\ &= -z \int \frac{\lambda}{\lambda(c-1 + czs_0(c, \mu) + czO_*(z)) + 1 - c) + z} d\zeta_d(\lambda) \\ &= -z \int \frac{\lambda}{\lambda(czs_0(c, \mu) + czO_*(z)) + z} d\zeta_d(\lambda) \\ &= - \int \frac{\lambda}{\lambda(cs_0(c, \mu) + cO_*(z)) + 1} d\zeta_d(\lambda). \end{aligned}$$

As per Assumption (2.2), $cO_*(z)$ is also uniformly bounded as $|cO_*(z)| \leq C(\tau)z$. Hence, $|\bar{G}_n(\mu, \zeta_d) - \bar{F}_n(z; \mu, \zeta_d)| \leq C(\tau) \|\beta_{oos}\| \|\beta_{is}\| z$.

3) Conclusion.

$$\begin{aligned}
|G_n - \bar{G}_n(\mu, \zeta_d)| &= |G_n - F_n(z) + F_n(z) - \bar{G}_n(\mu, \zeta_d)| \\
&\leq |G_n - F_n(z)| + |F_n(z) - \bar{G}_n(\mu, \zeta_d)| \\
&\leq |G_n - F_n(z)| + |F_n(z) - \bar{F}_n(z; \mu, \zeta_d) + \bar{F}_n(z; \mu, \zeta_d) - \bar{G}_n(\mu, \zeta_d)| \\
&\leq |G_n - F_n(z)| + |F_n(z) - \bar{F}_n(z; \mu, \zeta_d)| + |\bar{F}_n(z; \mu, \zeta_d) - \bar{G}_n(\mu, \zeta_d)| \\
&\leq C(\tau) \|\beta_{oos}\| \|\beta_{is}\| \left(z + \frac{1}{n^{1/2-\varepsilon} z} \right).
\end{aligned}$$

The last inequality follows from results 1) and 2) above and Lemma 2.

Taking $z = n^{-1/4} \geq n^{-2/3+\tau}$, we get

$$|G_n - \bar{G}_n(\mu, \zeta_d)| \leq \frac{C(\tau) \|\beta_{oos}\| \|\beta_{is}\|}{n^{1/4-\varepsilon}}$$

with probability $1 - n^{-D}$.

The proof of Lemma 9 is complete. □

Corollary 3. *Let Assumptions (2.1), (2.2), (A.1), (A.2), (A.3), (A.4), (A.6) and (A.7) hold. Then,*

$$G_n \xrightarrow{a.s.} \bar{G}_n(\nu, \eta_d) \quad (44)$$

Proof. Rewrite $G_n(\hat{\Sigma}, \Sigma) = G_n$ to highlight the dependence of the function on the sample covariance, $\hat{\Sigma}$, and the population covariance, Σ .

Note that

$$\begin{aligned}
|-z \langle \beta_{oos}, \Sigma_1(\hat{\Sigma} + zI)^{-1} \beta_{is} \rangle + z \langle \beta_{oos}, \Sigma_2(\hat{\Sigma} + zI)^{-1} \beta_{is} \rangle| &\leq z \|\beta_{is}\| \|\beta_{oos}\| \|(\hat{\Sigma} + zI)^{-1}\|_{\text{op}} \|\Sigma_1 - \Sigma_2\|_{\text{op}} \\
&\leq \|\beta_{is}\| \|\beta_{oos}\| \|\Sigma_1 - \Sigma_2\|_{\text{op}}
\end{aligned}$$

The second inequality follows after observing that $\|(\hat{\Sigma} + zI)^{-1}\|_{\text{op}} \leq z^{-1}$. This implies

$$|G_n(\hat{\Sigma}, \Sigma_1) - G_n(\hat{\Sigma}, \Sigma_2)| \leq \|\beta_{is}\| \|\beta_{oos}\| \|\Sigma_1 - \Sigma_2\|_{\text{op}}.$$

We also have

$$\begin{aligned}
&|-z \langle \beta_{oos}, \Sigma(\hat{\Sigma}_1 + zI)^{-1} \beta_{is} \rangle + z \langle \beta_{oos}, \Sigma(\hat{\Sigma}_2 + zI)^{-1} \beta_{is} \rangle| \\
&\leq z \|\beta_{is}\| \|\beta_{oos}\| \|\Sigma\|_{\text{op}} \|(\hat{\Sigma}_1 + zI)^{-1} - (\hat{\Sigma}_2 + zI)^{-1}\|_{\text{op}} \\
&\leq z\tau^{-1} \|\beta_{is}\| \|\beta_{oos}\| \|(\hat{\Sigma}_1 + zI)^{-1}(\hat{\Sigma}_1 + zI - (\hat{\Sigma}_2 + zI))(\hat{\Sigma}_2 + zI)^{-1}\|_{\text{op}} \\
&\leq z\tau^{-1} \|\beta_{is}\| \|\beta_{oos}\| \|(\hat{\Sigma}_1 + zI)^{-1}(\hat{\Sigma}_1 + zI - (\hat{\Sigma}_2 + zI))(\hat{\Sigma}_2 + zI)^{-1}\|_{\text{op}} \\
&\leq z\tau^{-1} \|\beta_{is}\| \|\beta_{oos}\| \|(\hat{\Sigma}_1 - \hat{\Sigma}_2)\|_{\text{op}} \|(\hat{\Sigma}_1 + zI)^{-1}\|_{\text{op}} z^{-1} \\
&\leq \tau^{-1} \|\beta_{is}\| \|\beta_{oos}\| \|(\hat{\Sigma}_1 - \hat{\Sigma}_2)\|_{\text{op}} \|(\hat{\Sigma}_1 + zI)^{-1}\|_{\text{op}}.
\end{aligned}$$

Let $\hat{\Sigma}_1 = n^{-1} X_1' X_1 = n^{-1} \Sigma^{1/2} Z_1' Z_1 \Sigma^{1/2}$. Then,

$$\begin{aligned}
& | -z\langle \beta_{oos}, \Sigma(\hat{\Sigma}_1 + zI)^{-1}\beta_{is} \rangle + z\langle \beta_{oos}, \Sigma(\hat{\Sigma}_2 + zI)^{-1}\beta_{is} \rangle | \\
& \leq \tau^{-1} \|\beta_{is}\| \|\beta_{oos}\| \|(\hat{\Sigma}_1 - \hat{\Sigma}_2)\|_{\text{op}} \frac{1}{\|\Sigma^{1/2}\|_{\text{op}}^2 \lambda_{\min}(n^{-1}Z_1'Z_1)} \\
& \leq \|\beta_{is}\| \|\beta_{oos}\| \|(\hat{\Sigma}_1 - \hat{\Sigma}_2)\|_{\text{op}} \frac{1}{\lambda_{\min}(n^{-1}Z_1'Z_1)}.
\end{aligned}$$

By Assumption (A.6), the Bai-Yin theorem (Bai and Yin (2008)) yields that $\lambda_{\min}(n^{-1}Z_1'Z_1) \geq \kappa(\tau) > 0$, almost surely. Hence,

$$| -z\langle \beta_{oos}, \Sigma(\hat{\Sigma}_1 + zI)^{-1}\beta_{is} \rangle + z\langle \beta_{oos}, \Sigma(\hat{\Sigma}_2 + zI)^{-1}\beta_{is} \rangle | \leq \kappa(\tau)^{-1} \|\beta_{is}\| \|\beta_{oos}\| \|(\hat{\Sigma}_1 - \hat{\Sigma}_2)\|_{\text{op}},$$

which implies

$$|G_n(\hat{\Sigma}_1, \Sigma) - G_n(\hat{\Sigma}_2, \Sigma)| \leq \kappa(\tau)^{-1} \|\beta_{is}\| \|\beta_{oos}\| \|(\hat{\Sigma}_1 - \hat{\Sigma}_2)\|_{\text{op}}.$$

Taking $C = \max \{ \|\beta_{is}\| \|\beta_{oos}\|, \kappa(\tau)^{-1} \|\beta_{is}\| \|\beta_{oos}\| \}$, the rest of the proof is similar to the one of Lemma 4. \square

Lemma 10. Let $\xi = (e_1, e_2, \dots, e_n)'$ with $(e_i)_i$ as in (1) and Assumptions (2.1), (2.2), (A.1), (A.6) and (A.7) hold. Besides, assume $\lambda_{\min}(n^{-1}Z'Z) \geq \kappa(\tau) > 0$, for any $n \in \mathbb{N}_{>0}$. Then, for $\varepsilon > 0$, there exist $C := C(\tau)$ such that with probability at least $1 - n^{-1/2}$,

$$\left| \frac{1}{n} \beta'_{oos} \Sigma \hat{\Sigma}^+ X' \xi \right| \leq \frac{C \|\beta_{oos}\|}{n^{1/4-\varepsilon}}.$$

Proof. Using Chebyshev's inequality, for some $t > 0$, we have

$$\mathbb{P} \left(\left| \frac{1}{n} \beta'_{oos} \Sigma \hat{\Sigma}^+ X' \xi \right|^2 \geq t \right) \leq \frac{\mathbb{V} \left[\frac{1}{n} \beta'_{oos} \Sigma \hat{\Sigma}^+ X' \xi \right]}{t^2} = \frac{\mathbb{E} \left[\left| \frac{1}{n} \beta'_{oos} \Sigma \hat{\Sigma}^+ X' \xi \right|^2 \right]}{t^2}. \quad (45)$$

The equality follows from the independence of X and ξ . Besides,

$$\begin{aligned}
\mathbb{E} \left[\left| \frac{1}{n} \beta'_{oos} \Sigma \hat{\Sigma}^+ X' \xi \right|^2 \right] &= \mathbb{E} \left[\left(\frac{1}{n} \beta'_{oos} \Sigma \hat{\Sigma}^+ X' \xi \right) \left(\frac{1}{n} \beta'_{oos} \Sigma \hat{\Sigma}^+ X' \xi \right)' \right] \\
&= \frac{1}{n^2} \mathbb{E} \left[\beta'_{oos} \Sigma \hat{\Sigma}^+ X' \xi \xi' X \hat{\Sigma}^+ \Sigma \beta_{oos} \right] \\
&= \mathbb{E} \left[\beta'_{oos} \Sigma \hat{\Sigma}^+ \frac{1}{n^2} \mathbb{E}[(X' \xi)(X' \xi)' | X] \hat{\Sigma}^+ \Sigma \beta_{oos} \right].
\end{aligned}$$

The last equality results from the law of iterated expectations. Next, using Lemma 5, we have

$$\begin{aligned}
\mathbb{E} \left[\left| \frac{1}{n} \beta'_{oos} \Sigma \hat{\Sigma}^+ X' \xi \right|^2 \right] &= \frac{1}{n} \mathbb{E} \left[\beta'_{oos} \Sigma \hat{\Sigma}^+ \hat{\Sigma} \hat{\Sigma}^+ \Sigma \beta_{oos} \right] \\
&= \frac{1}{n} \mathbb{E} \left[\beta'_{oos} \Sigma \hat{\Sigma}^+ \Sigma \beta_{oos} \right] \\
&\leq \frac{1}{n} \|\beta_{oos}\|^2 \|\Sigma\|_{\text{op}}^2 \frac{1}{\|\Sigma^{1/2}\|_{\text{op}}^2 \lambda_{\min}(n^{-1} Z' Z)} \\
&\leq \frac{1}{n} \|\beta_{oos}\|^2 \tau^{-3} \frac{1}{\lambda_{\min}(n^{-1} Z' Z)} \\
&\leq \frac{1}{n} C(\tau) \|\beta_{oos}\|^2.
\end{aligned} \tag{46}$$

Let $C := C(\tau)$ and $\varepsilon > 0$. Taking $t = C^{1/2} \|\beta_{oos}\| n^{-1/4+\varepsilon}$ in (45), we get

$$\mathbb{P} \left(\left| \frac{1}{n} \beta'_{oos} \Sigma (zI + \hat{\Sigma})^{-1} X' \xi \right| \geq \frac{C^{1/2} \|\beta_{oos}\|}{n^{1/4-\varepsilon}} \right) \leq \frac{1}{n^{1/2+2\varepsilon}}.$$

□

Corollary 4. Let $\xi = (e_1, e_2, \dots, e_n)'$ with $(e_i)_i$ as in (1) and Assumptions (2.1), (2.2), (A.1), (A.6) and (A.7) hold. Then,

$$\frac{1}{n} \beta'_{oos} \Sigma \hat{\Sigma}^+ X' \xi \xrightarrow{L_2} 0.$$

Proof. Using Bai-Yin theorem (Bai and Yin (2008)) and Assumption (A.6), we have $\limsup_{n,p \rightarrow \infty} \lambda_{\min}(n^{-1} Z' Z) \geq \kappa(\tau) > 0$. Then, the result follows from taking $n \rightarrow \infty$ in (46). □

Proposition 8. Let Assumptions (2.1), (2.2), (A.1), (A.2), (A.6) and (A.7) hold. Besides, assume $\lambda_{\min}(n^{-1} Z' Z) \geq \kappa(\tau) > \infty$, for any $n \in \mathbb{N}_{>0}$. Then, for $\varepsilon > 0$ and n sufficiently large, there exists $C := C(\tau)$ such that

$$\left| \lim_{z \rightarrow 0} \mathbb{E} \left[r_{t+1}^{(s)}(z) | X \right] - \left(\bar{H}_n(\zeta_d) + \bar{G}_n(\mu, \zeta_d) \mathbf{1}_{\{c>1\}} \right) \right| \leq \frac{C \|\beta_{is}\| \|\beta_{oos}\|}{n^{1/4-\varepsilon}} \tag{47}$$

holds with probability at least $1 - n^{-1/2}$.

Proof. Recall that

$$\mathbb{E} \left[r_{t+1}^{(s)}(z) | X \right] = \beta'_{oos} \Sigma (zI + \hat{\Sigma})^{-1} \hat{\Sigma} \beta_{is} + \frac{1}{n} \beta'_{oos} \Sigma (zI + \hat{\Sigma})^{-1} X' \xi.$$

If $c < 1$, $\lim_{z \rightarrow 0} \beta'_{oos} \Sigma (zI + \hat{\Sigma})^{-1} \hat{\Sigma} \beta_{is} = \beta'_{oos} \Sigma \beta_{is}$. Hence, from Lemma 10, we have

$$\left| \lim_{z \rightarrow 0} \mathbb{E} \left[r_{t+1}^{(s)}(z) | X \right] - \bar{H}_n(\zeta_d) \right| \leq \frac{C \|\beta_{is}\| \|\beta_{oos}\|}{n^{1/4-\varepsilon}}.$$

Next, note that

$$\begin{aligned}
\mathbb{E} \left[r_{t+1}^{(s)}(z) | X \right] &= \beta'_{oos} \Sigma (zI + \hat{\Sigma})^{-1} \hat{\Sigma} \beta_{is} + \frac{1}{n} \beta'_{oos} \Sigma (zI + \hat{\Sigma})^{-1} X' \xi \\
&= \beta'_{oos} \Sigma (zI + \hat{\Sigma})^{-1} (\hat{\Sigma} + zI - zI) \beta_{is} + \frac{1}{n} \beta'_{oos} \Sigma (zI + \hat{\Sigma})^{-1} X' \xi \\
&= \beta'_{oos} \Sigma \beta_{is} - z \beta'_{oos} \Sigma (zI + \hat{\Sigma})^{-1} \beta_{is} + \frac{1}{n} \beta'_{oos} \Sigma (zI + \hat{\Sigma})^{-1} X' \xi.
\end{aligned}$$

Thus, taking $D = 1/2$ in Lemma 9, we get

$$\left| \lim_{z \rightarrow 0} \mathbb{E} \left[r_{t+1}^{(s)}(z) | X \right] - \left(\bar{H}_n(\zeta_d) + \bar{G}_n(\mu, \zeta_d) \right) \right| \leq \frac{C \|\beta_{is}\| \|\beta_{oos}\|}{n^{1/4-\varepsilon}}.$$

□

We define the limiting out-of-sample expected return of the strategy under concept drift in the ridgeless case if the model is well-specified

$$\begin{aligned}
\mathcal{E}^{(d)}(c, \nu, \eta_d) &= \langle \beta_{oos}, \beta_{is} \rangle_R \\
&= \|\beta_{is}\| \|\beta_{oos}\| \int \left(\lambda - \frac{\lambda}{1 + \lambda c s_0(c, \mu)} \mathbb{1}_{\{c > 1\}} \right) d\eta_d(\lambda),
\end{aligned} \tag{48}$$

with

$$R \equiv R(c, \Sigma) := \begin{cases} \Sigma, & c < 1 \\ \Sigma(I - (c s_0(c, \mu) \Sigma + I)^{-1}), & c > 1 \end{cases}$$

and $s_0 := s_0(c, \mu)$ is given in Definition 5.

Proposition 9. *Let Assumptions (2.1), (2.2), (A.1), (A.2), (A.6), (A.7), (A.3) and (A.4) hold. Then,*

$$\mathbb{E} \left[r_{t+1}^{(s)}(z) | X \right] \xrightarrow[\substack{n, p \rightarrow \infty \\ p/n \rightarrow c \\ z \rightarrow 0}]{\mathbb{P}} \mathcal{E}^{(d)}(c, \nu, \eta_d).$$

Proof. Recall that

$$\mathbb{E} \left[r_{t+1}^{(s)}(z) | X \right] = \beta'_{oos} \Sigma (zI + \hat{\Sigma})^{-1} \hat{\Sigma} \beta_{is} + \frac{1}{n} \beta'_{oos} \Sigma (zI + \hat{\Sigma})^{-1} X' \xi.$$

If $c < 1$, $\lim_{z \rightarrow 0} \beta'_{oos} \Sigma (zI + \hat{\Sigma})^{-1} \hat{\Sigma} \beta_{is} = \beta'_{oos} \Sigma \beta_{is}$. Hence, the result in the underparameterized regime follows from Corollary 4.

Now, consider $c > 1$. By Lemma 3, we have

$$-z \beta'_{oos} \Sigma (zI + \hat{\Sigma})^{-1} \beta_{is} \xrightarrow[\substack{\text{a.s.} \\ n, p \rightarrow \infty \\ p/n \rightarrow c \\ z \rightarrow 0}]{-} -\beta_{oos} \Sigma (c s_0(c, \mu) \Sigma + I)^{-1} \beta_{is},$$

and by Corollary 4,

$$\frac{1}{n} \beta'_{oos} \Sigma \hat{\Sigma}^+ X' \xi \xrightarrow[n, p \rightarrow \infty]{p/n \rightarrow c} 0.$$

Consequently, for $c > 1$,

$$\mathbb{E} \left[r_{t+1}^{(s)}(z) | X \right] \xrightarrow[n, p \rightarrow \infty]{p/n \rightarrow c, z \rightarrow 0} \beta'_{oos} \Sigma \beta_{is} - \beta_{oos} \Sigma (cs_0(c, \mu) \Sigma + I)^{-1} \beta_{is}.$$

The proof of Proposition 9 is complete. \square

The next proposition establishes the limiting out-of-sample expected return of the strategy under concept drift in the ridgeless scenario when the covariates are i.i.d. with $\Sigma = I$ (isotropic features).

Proposition 10. *Assume $x_i = (x_{i1}, x_{i2}, \dots, x_{ip})$ has independent and identically distributed entries and, in addition, that for all $j \in \{1, \dots, p\}$, $\mathbb{E}[z_{ij}] = 0$, $\mathbb{E}[z_{ij}^2] = 1$ and $\mathbb{E}[|z_{ij}|^{4+a}] \leq C < \infty$ for $a > 0$. Then,*

$$\mathbb{E} \left[r_{t+1}^{(s)}(z) | X \right] \xrightarrow[n, p \rightarrow \infty]{p/n \rightarrow c, z \rightarrow 0} f(c) \langle \beta_{is}, \beta_{oos} \rangle$$

with

$$f(c) = 1 - \frac{c-1}{c} \mathbf{1}_{\{c>1\}} \in (0, 1]. \quad (49)$$

Proof. From (48), if $c < 1$, we have $\mathcal{E}^{(d)}(c, \nu, \eta_d) = \langle \beta_{is}, \beta_{oos} \rangle$. This yields the result in the underparameterized regime.

Now, consider $c > 1$. Again, from (48),

$$\mathcal{E}^{(d)}(c, \nu, \eta_d) = \left(1 - \frac{1}{1 + cs_0} \right) \langle \beta_{is}, \beta_{oos} \rangle, \quad (50)$$

and from Definition 5, we have

$$1 - \frac{1}{c} = \frac{1}{1 + cs_0},$$

which implies $s_0 = [c(c-1)]^{-1}$. Injecting this into (50), we get

$$\mathcal{E}^{(d)}(c, \nu, \eta_d) = \left(1 - \frac{c-1}{c} \right) \langle \beta_{is}, \beta_{oos} \rangle.$$

The proof of Proposition 10 is complete. \square

A.5.3 Misspecified model (General)

We now assume the data generating process (DGP) described in (1).

Proof of Proposition 2:

Let $x_t \in \mathbb{R}^p$ (resp. $w_t \in \mathbb{R}^q$) be a new independent sample of observable (resp. unobservable) features. Then,

$$\mathbb{E} \left[r_{t+1}^{(s,m)}(z) \middle| X \right] = \mathbb{E} \left[\hat{\pi}_t r_{t+1} \middle| X \right] \quad (51)$$

$$= \mathbb{E} \left[(\beta'_{oos} x_t + \theta'_{oos} w_t) x'_t \hat{\beta}_{is} \middle| X \right]. \quad (52)$$

Note that in the misspecified setting, we are also integrating over the randomness in the unobserved features W .

Similarly to (34) and by taking into account the presence of unobserved features, we can decompose $\hat{\beta}_{is}$ as follows

$$\begin{aligned} \hat{\beta}_{is} &= \frac{1}{n} (zI + \hat{\Sigma}_x)^{-1} X' (X \beta_{is} + W \theta_{is} + \xi) \\ &= (zI + \hat{\Sigma}_x)^{-1} (\hat{\Sigma}_x \beta_{is} + \hat{\Sigma}_{xw} \theta_{is} + \frac{1}{n} X' \xi). \end{aligned}$$

Therefore, coming back to (51),

$$\begin{aligned} \mathbb{E} \left[r_{t+1}^{(s,m)}(z) \middle| X \right] &= \mathbb{E} \left[(\beta'_{oos} x_t + \theta'_{oos} w_t) x'_t (zI + \hat{\Sigma}_x)^{-1} (\hat{\Sigma}_x \beta_{is} + \hat{\Sigma}_{xw} \theta_{is} + \frac{1}{n} X' \xi) \middle| X \right] \\ &= \beta'_{oos} \mathbb{E} \left[x_t x'_t \right] (zI + \hat{\Sigma}_x)^{-1} \hat{\Sigma}_x \beta_{is} \\ &\quad + \beta'_{oos} \mathbb{E} \left[x_t x'_t (zI + \hat{\Sigma}_x)^{-1} \hat{\Sigma}_{xw} \middle| X \right] \theta_{is} \\ &\quad + \frac{1}{n} \beta'_{oos} \mathbb{E} \left[x_t x'_t \right] (zI + \hat{\Sigma}_x)^{-1} X' \xi \\ &\quad + \theta'_{oos} \mathbb{E} \left[w_t x'_t \right] (zI + \hat{\Sigma}_x)^{-1} \hat{\Sigma}_x \beta_{is} \\ &\quad + \theta'_{oos} \mathbb{E} \left[w_t x'_t (zI + \hat{\Sigma}_x)^{-1} \hat{\Sigma}_{xw} \middle| X \right] \theta_{is} \\ &\quad + \frac{1}{n} \theta'_{oos} \mathbb{E} \left[w_t x'_t \right] (zI + \hat{\Sigma}_x)^{-1} X' \xi. \end{aligned}$$

By the law of iterated expectations, we have

$$\begin{aligned} \beta'_{oos} \mathbb{E} \left[x_t x'_t (zI + \hat{\Sigma}_x)^{-1} \hat{\Sigma}_{xw} \middle| X \right] \theta_{is} &= \beta'_{oos} \mathbb{E} \left[\mathbb{E} \left[x_t x'_t (zI + \hat{\Sigma}_x)^{-1} \hat{\Sigma}_{xw} \middle| X, W \right] \middle| X \right] \theta_{is} \\ &= \beta'_{oos} \mathbb{E} \left[\mathbb{E} \left[x_t x'_t \middle| X, W \right] (zI + \hat{\Sigma}_x)^{-1} \hat{\Sigma}_{xw} \middle| X \right] \theta_{is} \\ &= \beta'_{oos} \mathbb{E} \left[\Sigma_x (zI + \hat{\Sigma}_x)^{-1} \hat{\Sigma}_{xw} \middle| X \right] \theta_{is} \\ &= \beta'_{oos} \Sigma_x (zI + \hat{\Sigma}_x)^{-1} \mathbb{E} \left[\hat{\Sigma}_{xw} \middle| X \right] \theta_{is}, \end{aligned}$$

and

$$\begin{aligned}
\theta'_{oos} \mathbb{E} \left[w_t x'_t (zI + \hat{\Sigma}_x)^{-1} \hat{\Sigma}_{xw} \middle| X \right] \theta_{is} &= \theta'_{oos} \mathbb{E} \left[\mathbb{E} \left[w_t x'_t (zI + \hat{\Sigma}_x)^{-1} \hat{\Sigma}_{xw} \middle| X, W \right] \middle| X \right] \theta_{is} \\
&= \theta'_{oos} \mathbb{E} \left[\mathbb{E} \left[w_t x'_t \middle| X, W \right] (zI + \hat{\Sigma}_x)^{-1} \hat{\Sigma}_{xw} \middle| X \right] \theta_{is} \\
&= \theta'_{oos} \mathbb{E} \left[\Sigma'_{xw} (zI + \hat{\Sigma}_x)^{-1} \hat{\Sigma}_{xw} \middle| X \right] \theta_{is} \\
&= \theta'_{oos} \Sigma'_{xw} (zI + \hat{\Sigma}_x)^{-1} \mathbb{E} \left[\hat{\Sigma}_{xw} \middle| X \right] \theta_{is}.
\end{aligned}$$

Therefore,

$$\begin{aligned}
\mathbb{E} \left[r_{t+1}^{(s,m)}(z) \middle| X \right] &= \beta'_{oos} \Sigma_x (zI + \hat{\Sigma}_x)^{-1} \hat{\Sigma}_x \beta_{is} \\
&\quad + \beta'_{oos} \Sigma_x (zI + \hat{\Sigma}_x)^{-1} \mathbb{E} \left[\hat{\Sigma}_{xw} \middle| X \right] \theta_{is} \\
&\quad + \frac{1}{n} \beta'_{oos} \Sigma_x (zI + \hat{\Sigma}_x)^{-1} X' \xi \\
&\quad + \theta'_{oos} \Sigma'_{xw} (zI + \hat{\Sigma}_x)^{-1} \hat{\Sigma}_x \beta_{is} \\
&\quad + \theta'_{oos} \Sigma'_{xw} (zI + \hat{\Sigma}_x)^{-1} \mathbb{E} \left[\hat{\Sigma}_{xw} \middle| X \right] \theta_{is} \\
&\quad + \frac{1}{n} \theta'_{oos} \Sigma'_{xw} (zI + \hat{\Sigma}_x)^{-1} X' \xi.
\end{aligned}$$

The proof of Proposition 2 is complete. \square

A.5.4 Misspecified model (Isotropic features)

Proof of Proposition 3:

$\Sigma = I$, then $\Sigma_{xw} = 0$. Moreover, as X and W are independent and $\mathbb{E}[W] = 0$, we have

$$\mathbb{E} \left[\hat{\Sigma}_{xw} \middle| X \right] = \frac{1}{n} X' \mathbb{E} [W \middle| X] = \frac{1}{n} X' \mathbb{E} [W] = 0$$

Consequently,

$$\begin{aligned}
\mathcal{M}(z) &= \left(\beta'_{oos} \Sigma_x + \theta'_{oos} \Sigma'_{xw} \right) (zI + \hat{\Sigma}_x)^{-1} \mathbb{E} \left[\hat{\Sigma}_{xw} \middle| X \right] \theta_{is} \\
&\quad + \theta'_{oos} \Sigma'_{xw} (zI + \hat{\Sigma}_x)^{-1} \left(\hat{\Sigma}_x \beta_{is} + \frac{1}{n} X' \xi \right) \\
&= 0.
\end{aligned}$$

Finally, we end up in the same setting as Proposition 7 where the complexity ratio is now the misspecified one, i.e. $c\phi$. \square

A.5.5 Misspecified model (Latent space model)

We can also consider a latent space model as presented in [Hastie et al. \(2020\)](#) and [Misiakiewicz and Montanari \(2023\)](#). This model will allow us to highlight a situation where the expected returns of the strategy depend on the alignment between the eigenvectors of the population covariance matrix and the true vector of regression coefficients. Remark that this symmetry plays no role when the features are isotropic (see [Appendix A.5.4](#), e.g.).

Namely, we consider a model in which the dependent variable is linear in a latent covariate vector, $z_i \in \mathbb{R}^d$. Though, we are only able to observe a vector of $p(\geq d)$ covariates, x_i , whose components are linear in the latent features. Formally,

$$\begin{aligned} (z_i, b_i, u_i) &\sim \mathcal{N}(0, I_d) \times \mathcal{N}(0, \sigma_b^2) \times \mathcal{N}(0, 1), \quad i = 1, \dots, n \\ y_i &= z_i' \theta + b_i, \quad i = 1, \dots, n, \\ x_i &= W z_i + u_i, \quad i = 1, \dots, n, \end{aligned} \tag{53}$$

where the n random draws are independent. $(b_i)_{1 \leq i \leq n}$ and $(u_{ij})_{1 \leq i \leq n, 1 \leq j \leq p}$ are independent. Moreover, the latent covariates, z_i , are independent from both noise variables. $W \in \mathbb{R}^{p \times d}$ is the linear transformation relating the observed features to the latent covariates.

DGP (53) is a special case of DGP (1) where $w_i = 0$, $P_x \sim \mathcal{N}(0, \Sigma)$ and $P_e \sim \mathcal{N}(0, \sigma^2)$. Formally, this new DGP can be written

$$\begin{aligned} (x_i, e_i) &\sim \mathcal{N}(0, \Sigma) \times \mathcal{N}(0, \sigma^2), \quad i = 1, \dots, n \\ y_i &= x_i' \beta + e_i, \quad i = 1, \dots, n. \end{aligned}$$

It is straightforward that $\Sigma = \mathbb{E}[x_i x_i'] = \mathbb{E}[(W z_i + u_i)(W z_i + u_i)'] = I + W W'$. Further, taking $\beta = W(I + W'W)^{-1} \theta$ and $e_i = b_i + \theta'(I + W'W)^{-1}(z_i - W' u_i)$ yields $y_i = z_i' \theta + b_i$. Hence, $\sigma^2 = \mathbb{E}[e_i^2] = \sigma_b^2 + \theta'(I + W'W)^{-1} \theta$.

Let $\Upsilon = d/p \in (0, 1)$. For the sake of simplicity, we also consider W to be proportional to an orthogonal matrix, i.e. $W'W = \Upsilon^{-1} I_d$.

Proposition 11. *Let $z > 0$. Assume the data is generated as per (53). Then,*

$$\mathbb{E} \left[r_{t+1}^{(s)}(z) \middle| X \right] \xrightarrow[\substack{n, p, d \rightarrow \infty \\ p/n \rightarrow c \\ d/p \rightarrow \Upsilon}]{\mathbb{P}} g(z; c, \Upsilon) \langle \theta_{is}, \theta_{oos} \rangle$$

with

$$g(z; c, \Upsilon) = \frac{1}{1 + \Upsilon} \left(1 - \frac{z}{(1 + \Upsilon^{-1})(c z m_n + 1 - c) + z} \right)$$

and $m_n := m_n(-z; c, \Upsilon)$ the unique solution in \mathbb{C}_+ to

$$m_n = \frac{1 - \Upsilon}{1 - c + c z m_n + z} + \frac{\Upsilon}{(1 + \Upsilon^{-1})(1 - c + c z m_n) + z}$$

Moreover, in the ridgeless limit,

$$\mathbb{E} \left[r_{t+1}^{(s)}(z) \middle| X \right] \xrightarrow[\substack{n,p,d \rightarrow \infty \\ p/n \rightarrow c \\ d/p \rightarrow \Upsilon \\ z \rightarrow 0}]{\mathbb{P}} g(c, \Upsilon) \langle \theta_{is}, \theta_{oos} \rangle$$

with

$$g(c, \Upsilon) = \lim_{z \rightarrow 0} g(z; c) = \frac{1}{1 + \Upsilon} \left(1 - \frac{1}{1 + (1 + \Upsilon^{-1})cs_0} \mathbb{1}_{c > 1} \right)$$

and $s_0 := s_0(c, \Upsilon)$ the non-negative solution to

$$1 - \frac{1}{c} = \frac{1 - \Upsilon}{1 + cs_0} + \frac{\Upsilon}{1 + c(1 + \Upsilon^{-1})s_0}$$

Proof. First, we need to determine the measures μ and ζ_d . Note that Σ admits the following eigenvalue decomposition

$$\Sigma = PDP' + I_p = \sum_{i=1}^d (1 + \Upsilon^{-1})v_i v_i' + \sum_{i=d+1}^p v_i v_i', \quad (54)$$

with $(v_i)_{1 \leq i \leq d}$ the columns of $P \in \mathbb{R}^{p \times d}$ and, for $d+1 \leq i \leq p$, v_i is a canonical basis vector with 1 in position i .

Σ has d eigenvalues equal to $1 + \Upsilon^{-1}$ and $p - d$ equal to 1, hence

$$\mu = \Upsilon \delta_{1+\Upsilon^{-1}} + (1 - \Upsilon) \delta_1$$

Next, let W admit the following singular value decomposition

$$W = PDQ'$$

with $P \in \mathbb{R}^{p \times d}$ and $Q \in \mathbb{R}^{d \times p}$ orthogonal and $D \in \mathbb{R}^{d \times p}$ such that

$$D_{ij} = \begin{cases} \Upsilon^{-1/2}, & i = j \\ 0, & i \neq j. \end{cases}$$

Then,

$$\begin{aligned} \langle \beta, v_i \rangle^2 &= \beta' v_i v_i' \beta \\ &= (1 + \Upsilon^{-1})^{-2} \theta' W' v_i v_i W \theta \\ &= (1 + \Upsilon^{-1})^{-2} \theta' Q D' P' v_i v_i' P D Q' \theta \end{aligned}$$

$P' v_i = v_i' P = (v_1' v_i, v_2' v_i, \dots, v_d' v_i)'$ which is equal to the canonical basis vector with 1 in position i if $i \leq d$ or to the null vector if $d+1 \leq i \leq p$.

Then, for $u \in \{is, oos\}$, we have

$$\begin{aligned}
\zeta_u &= \frac{1}{\|\beta_u\|^2} \sum_{i=1}^p |\langle \beta_u, v_i \rangle|^2 \delta_{\lambda_i} \\
&= \frac{1}{\|\beta_u\|^2} \left(\sum_{i=1}^d |\langle \beta_u, v_i \rangle|^2 \delta_{1+\Upsilon^{-1}} + \sum_{i=d+1}^p |\langle \beta_u, v_i \rangle|^2 \delta_1 \right) \\
&= \frac{1}{\|\beta_u\|^2} \beta_u' \left(\sum_{i=1}^d v_i v_i' \right) \beta_u \delta_{1+\Upsilon^{-1}} \\
&= \frac{1}{\|\beta_u\|^2} \beta_u' \beta_u \delta_{1+\Upsilon^{-1}} \\
&= \delta_{1+\Upsilon^{-1}}.
\end{aligned}$$

Similarly, $\zeta_r = \delta_{1+\Upsilon^{-1}}$. Note that $\|\beta_u\|^2 = \Upsilon(1 + \Upsilon)^{-2} \|\theta_u\|^2$. Hence,

$$\begin{aligned}
\zeta_d &= \frac{1}{2\|\beta_{is}\| \|\beta_{oos}\|} \left(\|\beta_{is}\|^2 \zeta_{is} + \|\beta_{oos}\|^2 \zeta_{oos} - \|\beta_{oos} - \beta_{is}\|^2 \zeta_r \right) \\
&= \frac{1}{2\|\theta_{is}\| \|\theta_{oos}\|} \left(\|\theta_{is}\|^2 + \|\theta_{oos}\|^2 - \|\theta_{oos} - \theta_{is}\|^2 \right) \delta_{1+\Upsilon^{-1}} \\
&= \frac{\langle \theta_{is}, \theta_{oos} \rangle}{\|\theta_{is}\| \|\theta_{oos}\|} \delta_{1+\Upsilon^{-1}}
\end{aligned}$$

From there, the result in the ridge regularization scenario follows from Proposition 5 and Definition 4 while the result for the ridgeless limit is a direct application of Proposition 9 and Definition 5.

The proof of Proposition 11 is complete. □